

New diagnostic and therapeutical possibilities in the treatment of glioblastoma multiforme

Ph.D Theses

Dr. Bellyeine Dr. Pozsgai Eva

University of Pecs, Department of Clinical Chemistry and Biochemistry

Program leader: Prof. Dr. Sumegi Balazs

2011.

Introduction

Malignant gliomas, such as glioblastoma multiforme, are the most frequent type of primary brain tumors [1]. They can be typified by diffuse infiltration of the brain and increased resistance to conventional cancer therapies [1]. The standard approach of treatment is multimodal: surgical resection is followed by adjuvant radiotherapy and chemotherapy, with the alkylating agent temozolomide [2]. Recent studies investigating the genetic alterations as well as the disordered tumor proliferation signaling pathways underlying glioma formation may aid diagnosis and lead to the development of more tailored therapies in non-responding cases [3]. Antiangiogenic therapy with antivascular endothelial growth factor antibodies (bevacizumab) is an example of targeted-therapy that has been introduced for the treatment of recurrent or progressive glioblastoma [4]. Despite notable advancements in oncology, however, the early diagnosis and successful treatment of malignant gliomas continues to present a great challenge [5].

Heat shock proteins (Hsp) are a ubiquitous group of proteins found in all living organisms. They are expressed in response to different types of stress including environmental changes and the stages of development. Hsp also function as molecular chaperones aiding the folding and assembly of proteins and their refolding or –in some cases- elimination, if the damage done to the protein is irreversible. Hence, Hsp play an important role in cytoprotection and cell survival [6].

Small Hsps (sHsp) have a molecular weight ranging between 2-43 kDa. They comprise a structurally divergent group characterized by a conserved sequence of 80-100 amino acid residues called the alpha-crystallin domain, which is flanked by two extensions. The N-terminal extension is poorly conserved and is responsible for oligomer construction and chaperone activity, whereas the C-terminal is a highly variable, flexible region accountable for stabilizing the quaternary structure and enhancing protein/substrate complex solubility. sHsp also contain a highly conserved arginine, whose characterization was of particular importance since the residues' mutation has been found to contribute to some diseases [7; 8].

Although the molecular mass of sHsps does not exceed 43 kDa, they assemble into large complexes up to 1 MDa. Beta-strands account mostly for the secondary structure with little alpha-helical content. Dimer formation is brought about by beta-sheets within the alpha-crystallin domain [8; 9].

Like other Hsp, small stress proteins also act as molecular chaperones. They increase the cells' resistance to stress by suppressing the aggregation of denatured proteins or by storing aggregation prone proteins. The amount of sHsp in a cell and their localization inside the cell differs according to the lack or presence of physiological stressors, like heat, hypoxia or cell development [7].

Our knowledge of sHsps is rather limited, however their apparently significant role have made them a target for research recently. The two most studied sHsps have been alphaB-crystallin and Hsp 27 [8; 9]. AlphaB-crystallin is a major soluble protein found in vertebrate eye lenses, however it is present in other, non-ocular tissues (e.g. skeletal muscle, kidney, heart muscle) as well. Hsp 27 was originally identified in human MCF-7 cells and human breast carcinomas as being identical with the 24-kD protein. Later Hsp 27 was found to be expressed in other malignancies as well [10].

It follows, from the central role of sHsps, that inappropriate change in their structure or function – due to mutation in their DNA- is likely to lead to the damage of the cell and finally, to the development of a disease. sHsps have the potential to guard cells from damage and disease but when they are disturbed or are present in tumorous cells, they can foster disease. Thus, sHsps have been linked to various human illnesses [7].

It is particularly worthwhile to examine the role of sHsps in cancer. The discovery that a positive correlation exists between the levels of alphaB-crystallin and lymph node involvement in breast cancer turned the attention of researchers towards the possibility of sHsps being used as tumor markers [7].

Previously, while searching NCBI database, our working group noticed a homology between the amino acid sequences of C1ORF41 and alphaB-crystallin. Since small heat shock proteins are homologous to alphaB-crystallin [11], it raised the possibility that C1ORF41 may have a physiological role similar to that of small heat shock proteins. To indicate this putative physiological role, we used the name small heat shock protein 16.2 (Hsp16.2) for C1ORF41 further on. Consequent experiments, such as the induction of its synthesis to heat stress and its ATP-independent chaperone activity, indicated that Hsp16.2 is a novel small heat shock protein. Suppression of Hsp16.2 sensitized cells to apoptotic stimuli, while over-expressing of Hsp16.2 protected cells against H₂O₂ and taxol induced cell death. Under stress conditions, Hsp16.2 inhibited the release of cytochrome c from the mitochondria, nuclear translocation of AIF and endonuclease G, and caspase 3 activation by protecting the integrity of mitochondrial membrane system. Furthermore, Hsp16.2 was found to bind to Hsp90, thus Hsp16.2 mediated cytoprotection requires Hsp90 activation. Hsp16.2 over-

expression facilitated lipid rafts formation, and increased Akt phosphorylation (ser-473) supporting the idea that stabilization of lipid rafts is essential to Akt activation [D48]. The inhibition of PI-3-kinase-Akt pathway by LY-294002, or wortmannin, significantly decreased its protective effect. Taken together, these data indicated that one of the main mechanisms by which Hsp16.2 inhibits cell death is the activation of Hsp90 followed by activation of lipid raft formation and by the activation of PI-3-kinase - Akt cytoprotective pathway .

Preliminary studies indicated that Hsp16.2 is expressed in neuroectodermal tumors. Despite the number of recent findings, none of the sHsps' have yet been correlated with a *wide range* of brain tumor types –only with astrocytic brain cancers- and none have shown the exact correlation with the *different grades* of brain tumors (grade1,2,3 and 4).

Therefore, we began to study the expression of Hsp 16.2 in different types of brain tumors including benign and malignant meningioma, oligodendroglioma, glioblastoma multiforme, ependymoma and medulloblastoma. Our aim was to examine whether Hsp16.2 plays a part in the development of various types of brain tumors and whether the level of its expression correlates with the malignancy of the tumor.

Growth hormone-releasing hormone (GHRH) is a peptide hormone secreted by the hypothalamus [12]. GHRH induces growth hormone (GH) secretion after binding to pituitary-type GHRH receptors (pGHRH-R) in the anterior pituitary [13; 14; 15; 16]. The insulin-like growth factor I (IGF-I) stimulated by GH, plays an important role in the mechanism of malignant transformation, metastasis and tumorigenesis in various cancers, including brain cancers [14; 17; 18]. The detection of mRNA for GHRH in malignant gliomas indicates that GHRH also plays a role in the pathogenesis of this tumor [19; 20]. The presence of pGHRH-R and its splice variant with a high structural homology to pGHRH-R, SV1, on DBTRG-05 glioblastoma cancer cell line has also been previously demonstrated [21]. GHRH antagonists have been applied successfully for the treatment of different types of experimental tumors, including malignant gliomas based on their ability to block the secretion of GH, thereby suppressing the hepatic production of IGF-I [12; 19]. The efficacy of GHRH antagonists is also due to the blocking of the binding of autocrine GHRH to receptors on tumor cells, without an involvement of IGFs [13; 20]. GHRH antagonists could provide a potential treatment for glioblastomas, since their passage across the blood-brain barrier and accumulation in the brain have been proved [22].

The effects of the GHRH antagonists' on cancer cell viability and cell signaling pathways have not yet been elucidated. In the present study, we investigated the mechanism of action of two new potent GHRH antagonists: JMR-132 and MIA-602. Our goal was to

examine the signal transduction and cellular response of brain tumor cells to treatment with GHRH antagonists and to investigate the effectiveness of GHRH antagonist MIA-602 *in vivo*.

The inhibitory effects of GHRH antagonists on tumor growth, invasion and metastatic ability of various cancers *in vivo* have previously been investigated [23; 24; 25]. However, the actions of the new GHRH antagonist, MIA-602 on metastatic potential, and cellular mechanisms affected, have not yet been described. In our *in vitro* study in three highly malignant cell lines including the glioblastoma cell line, DBTRG-05, it was our goal to demonstrate how MIA-602 affects the critical steps of malignant tumorigenesis, such as cell proliferation, stimulation of angiogenesis, enhancement of cell motility, cellular invasion and the production of key proteins involved in metastasis development.

Taken together, the aims of my study were to determine the following:

1. Is Hsp 16.2 present in different types of brain tumors?
2. Can a correlation be found between the expression of Hsp 16.2 and the grades of different brain tumors?
3. Are the pGHRH receptor and its main splice variant, SV1, expressed in glioblastoma cell lines?
4. Do GHRH antagonists have an effect on the cell survival of glioblastoma cell lines?
5. Do GHRH antagonists have an effect on the cell signalling pathways of glioblastoma cell lines?
6. How do GHRH antagonists influence the mitochondrial membrane potential of glioblastoma cells?
7. Do GHRH antagonists decrease the rate of glioblastoma tumor growth in a nude mouse animal model?
8. Do GHRH antagonists have an effect on invasion and metastasis development *in vitro*?
9. Could GHRH antagonists be a possible therapeutic tool for the treatment of malignant gliomas?

Materials and Methods

(for the study regarding Hsp 16.2)

Tumor materials

Brain tumor samples from fifty-one patients were available for examination. All tumor tissue specimens were provided by the Medical University of Pécs, Department of Neurosurgery and Pathology. Full ethical approval was given by the local Ethics Committee for the use of these samples. Each type of tumor was identified according to the revised WHO classification on Histological Typing of the Tumors of the Central Nervous System [10].

Preparation of polyclonal antibodies against Hsp16.2.

Rabbits were immunized subcutaneously at multiple sites with 100 µg of recombinant Hsp16.2/GST fusion protein in Freund's complete adjuvant. Four subsequent booster injections at 4-week intervals were given with 50 µg of protein in Freund's incomplete adjuvant. Blood was collected 10 days after boosting, and the antisera were stored at -20°C. IgGs were affinity purified from the sera by protein G-Sepharose chromatography according to the manufacturer's protocol.

Immunohistochemistry

Sections from the tumor tissue samples were formalin-fixed and paraffin-embedded. Subsequently, they were incubated with polyclonal anti-Hsp16.2 polyclonal antibody. Immunohistochemical staining was carried out according to the streptavidin-biotin-peroxidase method with hydrogen peroxide/3-amino-9-ethylcarbazole development using the Universal kit. Only secondary IgG was incubated with the control sections. The evaluation of the slides was done with the help of an Olympus BX50 light microscope with incorporated photography system (Olympus Optical Co., Hamburg, Germany). Both the presence and localization of positive staining for Hsp16.2 was examined. Staining intensity was recorded semiquantitatively as mild (+), moderate (++) or strong (+++), following as it was described before [9/24]. For internal positive control, the normal cerebral and vascular structures of the samples were used. Positive areas around necrotic fields were excluded due to their probable stress related up-regulation.

Immunoblot analysis

Tumor tissue specimens were homogenized in chilled lysis buffer of 0,5 mM sodium metavanadate, 1 mM EDTA, and protease inhibitor mixture in phosphate-buffered saline in a Teflon/glass homogenizer, and centrifuged. Isolation of cytosol and nuclear fractions were carried out by standard lab protocols exactly as previously [9/23]. The samples were equalized to 1 mg/ml total protein concentration using Biuret's method and subjected to SDS-PAGE. Proteins (20µg/lane) were separated on 15% gels and then transferred to nitrocellulose membranes. The membranes were blocked in 5% low fat milk for 1 h at room temperature, then exposed to the primary anti-Hsp16,2 antibodies at 4 °C overnight at a dilution of 1:2,000 in blocking solution. Appropriate horseradish peroxidase-conjugated secondary antibodies were used for 2 h at room temperature and at 1:5,000 dilution. Peroxidase labeling was visualized with enhanced chemiluminescence (ECL) using an ECL Western blotting detection system (Amersham Biosciences). The developed films were scanned, and the pixel volumes of the bands were determined using NIH Image J software. All experiments were repeated four times.

Statistical analysis

Difference in distribution of variables between groups was tested using χ^2 test. Values of $p < 0.01$ were considered to be significant.

(for experiments regarding the mechanism of action of GHRH antagonists)

Peptides and chemicals

GHRH antagonists JMR-132 and MIA-602 were synthesized in our laboratory by solid-phase method and purified by reversed-phase HPLC as described previously(10^{/18}). The

chemical structure of JMR-132 is [PhAc⁰-Tyr¹, D-Arg², Cpa⁶, Ala⁸, Har⁹, Tyr(Me)¹⁰, His¹¹, Abu¹⁵, His²⁰, Nle²⁷, D-Arg²⁸, Har²⁹]hGH-RH(1-29)NH₂, and the structure of MIA-602 is [(PhAc-Ada)⁰-Tyr¹, D-Arg², Fpa⁵, Ala⁸, Har⁹, Tyr(Me)¹⁰, His¹¹, Orn¹², Abu¹⁵, His²⁰, Orn²¹, Nle²⁷, D-Arg²⁸, Har²⁹]hGH-RH(1-29)NH₂. Non-coded amino acids and acyl groups used in the antagonists are abbreviated as follows: Abu, α -aminobutyric acid; Ada, 12-aminododecanoic acid; Cpa, *para*-chlorophenylalanine; Fpa5, pentafluoro-phenylalanine; Har, homoarginine; Nle, norleucine; Orn, ornithine; PhAc, phenylacetyl; Try(Me), O-methyl-tyrosine. GHRH(1-29)NH₂ was also synthesized in our laboratory. For daily injection, GHRH antagonists were dissolved in 0.1% DMSO (Sigma) in 10% aqueous propylene glycol (vehicle solution). For in vitro experiments, GHRH(1-29)NH₂ and GHRH antagonists were dissolved in 0.1% DMSO and diluted with incubation media.

Cell lines and animals

The cell lines (DBTRG-05, U-87MG and NIH/3T3) were obtained from American Type Culture Collection (Manassas, VA, USA) and cultured at 37 °C in a humidified 95% air/5% CO₂ atmosphere. DBTRG-05 cells were cultured in RPMI-1640 supplemented with antibiotics/antimycotics, 10% FBS and HEPES. U-87 cells were cultured in EMEM and NIH/3T3 cells in DMEM, supplemented with antibiotics/antimycotics and 10% FBS. The culture media were purchased from GIBCO (Carlsbad, CA).

Five- to 6-week-old male athymic nude mice (*Ncr nu/nu*) were obtained from the National Cancer Institute (Bethesda, MD). The animals were housed in sterile cages under laminar flow hoods in a temperature-controlled room with a 12-h light/12-h dark schedule. They were fed autoclaved chow and water ad libitum. Donor mice were injected subcutaneously with 1×10^6 glioblastoma DBTRG-05 cells. After 3 weeks, tumor tissue grown in donor animals was minced and passed through a wire mesh. A suspension of 150 μ l was injected s.c. into experimental nude mice. The experiment was initiated when DBTRG-05 tumors had reached a volume of approximately 70 mm³. Mice were divided into two experimental groups of 10 animals each: group 1, control; group 2, MIA-602 s.c. at a dose of 5 μ g/day. Tumor volume (length \times width \times height \times 0.5236) and body weight also were measured weekly. The trial was ended 4 weeks after the initiation of the treatment, mice were killed under anesthesia, and necropsy was performed. Tumors and organs were removed and weighed. All experiments were conducted in accordance with the institutional guidelines for the welfare of animals in experiments. The Institutional Animal Care and Use Committee of the VA medical Center in Miami approved the protocols.

Proliferation assay

Cells were seeded onto 96-well-plates at a starting density of 2500 cells/well, cultured overnight, starved for 24 hours with medium containing no FBS and then treated with GHRH (1-29)NH₂ or GHRH antagonist in a medium containing 0.5% FBS for 48 hours. After the treatment, the relative number of viable cells was measured in comparison with the untreated control and the solvent control using Cell Titer 96 AQueous Assay (Promega) according to the manufacturer's instructions at 490 nm in a Victor3 multilabel counter (Perkin-Elmer, Waltham, MD, USA). All experiments were done at least in quadruplicate and repeated three times. The percentage of cell survival was determined by comparing the absorbance value of the vehicle control.

Isolation of subcellular fractions

Cells were pre-starved for 24 hours in serum free medium, then treated with GHRH antagonists or GHRH(1-29)NH₂ at a concentration of 1 μ M, for the time periods

demonstrated in the results section (5, 10, 30 minutes, 6 and 24 hours, respectively). Cells were harvested and centrifuged at low-speed, then the pellet was dispersed by vortexing in lysis buffer (50mM Tris-HCl (pH=8.0), 1% Triton X-100, 10% glycerol, 1mM EDTA, 250mM NaCl, 1mM dithiothreitol, 1mM phenylmethylsulfonylfluoride, 2mM sodium vanadate, 100mM sodium fluoride, 10 mg/ml aprotinin, 10 mg/ml leupeptin and 10 mg/ml pepstatin) for 10 min at 4 °C. Isolation of cytosol, nuclear and mitochondrial fractions was carried out by standard lab protocols as described previously [26].

Western blot

Cells were washed with PBS, and directly lysed in lysis buffer. Cell lysates were adjusted to equal protein concentrations (NanoDrop Technologies, Inc., Wilmington, DE), resuspended in 2X sample loading buffer containing 4% SDS, 20% glycerol, 120mM Tris and bromophenol blue, and were boiled for 5 min. Protein samples were subjected to SDS-polyacrylamide gel electrophoresis. Proteins on the gel were transferred onto nitrocellulose membranes that were blocked with 50-50% Odyssey buffer and phosphate buffered saline (PBS) for 1 h at room temperature. Afterwards, the membranes were incubated with the indicated primary antibodies overnight at 4 °C. GHRH-R primary antibody was purchased from Abcam, Cat. No.: ab28692 (Abcam Inc., Cambridge, MA). p-AKT, p-ERK1/2, pGSK3 β , phospho-p38, Poly(ADP-ribose) (PARP), caspase-3, cleaved PARP, cleaved caspase-3, cytochrom c (cyt c), apoptosis inducing factor (AIF) and endonuclease G (Endo G) primary antibodies were purchased from Cell Signaling. α -tubulin primary antibody was obtained from Calbiochem. After washing with PBS containing 0.1% Tween-20, the membranes were incubated with the appropriate secondary antibody. The immunoreactive bands were visualized with the Odyssey Infrared Imaging System and V. 3.0 software was used (LI-COR Biosciences, Lincoln, Nebraska).

Fluorescent microscopy

DBTRG-05 cells were seeded to cover slips. After subjecting the cells to the treatment indicated in the figure legends, live imaging by using JC-1 dye was performed exactly as described previously (10¹⁹). The fluorescence microscope and software used were made by Nikon Instruments Inc., Lewisville, TX and NIS-ELEMENTS BR software.

Statistical analysis

Results are expressed as means \pm SE. Results were compared using Student's t test, P < 0.05 being accepted as statistically significant.

(for experiments regarding the reduction of invasion- and metastasis- potential of cancer cells by GHRH antagonists)

Peptides and chemicals

GHRH antagonist MIA-602 was synthesized in our laboratory by solid-phase method and purified by reversed-phase HPLC as described previously [27]. The chemical structure of MIA-602 is [(PhAc-Ada)⁰-Tyr¹, D-Arg², Fpa⁵, Ala⁸, Har⁹, Tyr(Me)¹⁰, His¹¹, Orn¹², Abu¹⁵, His²⁰, Orn²¹, Nle²⁷, D-Arg²⁸, Har²⁹]hGH-RH(1-29)NH₂. Non-coded amino acids and acyl groups used in the antagonists are abbreviated as follows: Abu, α -aminobutyric acid; Ada, 12-aminododecanoic acid; Fpa5, pentafluoro-phenylalanine; Har, homoarginine; Nle, norleucine; Orn, ornithine; PhAc, phenylacetyl; Try(Me), O-methyl-tyrosine. For the experiments the GHRH antagonist was dissolved in 0.1% DMSO and diluted with incubation media.

Cell lines

The human cell lines (DBTRG-05 glioblastoma, MDA-MB-468 estrogen independent breast cancer, and ES-2 clear cell ovarian cancer) were obtained from American Type Culture Collection (Manassas, VA, USA) and cultured at 37 °C in a humidified 95% air/5% CO₂ atmosphere. DBTRG-05 cells were cultured in RPMI-1640 supplemented with antibiotics/antimycotics, 10% FBS and HEPES. MDA-MB-468 cells were cultured in DMEM and ES-2 cells in McCoy's 5A, supplemented with antibiotics/antimycotics and 10% FBS. The culture media were purchased from GIBCO (Carlsbad, CA).

Proliferation assay

Cells were seeded onto 96-well-plates at a starting density of 2500 cells/well, cultured overnight, starved for 24 hours with medium containing no FBS and then treated with 1 μM GHRH antagonist MIA-602 for 48 hours. After the treatment the relative number of viable cells were measured in comparison with the untreated control and the solvent control using Cell Titer 96 AQueus Assay (Promega) according to the manufacturer's instructions at 490 nm in a Victor3 multilabel counter (Perkin-Elmer, Waltham, MD, USA). All experiments were run at least in quadruplicate and repeated three times. The percentage of cell survival was determined by comparing the absorbance value of the vehicle control.

Adhesion assay

The adhesion assay was performed by MTT assay. All three cell lines were starved for 24 hours with medium containing no FBS. Then monolayers of the cell lines (1×10^5) were incubated with or without 1 μM GHRH antagonist MIA-602 for 24 hours. Subsequently, the cells were planted into the fibronectin-precoated (10 μg/ml) and matrigel-precoated (100 μg/ml) 96-well plate in triplicate. The groups of cells were washed at 30 min, 60 min and 90 min, respectively, to remove the non-adherent cells. After washing, the adhered cells were measured by MTT assay at 490 nm. The OD values of washed groups compared with those of non-washing groups reflect the proportion of cells adhered to the fibronectin and matrigel-coated 96-well plate.

Gelatin zymography

DBTRG-05, MDA-MB-468, and ES-2 cell lines were starved for 24 hours with medium containing no FBS. Subsequently, the cells in media containing 0.5% FBS were stimulated with 1 μM GHRH antagonist MIA-602 for different time periods and then, the supernatants were collected. The samples were analyzed with gelatin zymography, (0.1% w/v) gelatin (Sigma) as the substrate. Each lane was loaded with a total protein concentration of 3 μg and subjected to SDS-PAGE electrophoresis at 48 °C. Gels were washed twice in 50 mM Tris (pH 7.4) containing 2.5% (v/v) Triton X-100 for 1 hr, followed by two 10-min rinses in 50 mM Tris (pH 7.4). After SDS removal, the gels were incubated overnight in 50 mM Tris (pH 7.5) containing 10 mM CaCl₂, 0.15 M NaCl, 0.1% (v/v) Triton X-100, and 0.02% sodium azide at 37°C under constant gentle shaking. After incubation, the gels were stained with 0.25% Coomassie brilliant blue R-250 (Sigma) and destained in 7.5% acetic acid with 20% methanol. The gelatinase bands appeared white on a blue background. The activity of metalloproteinases MMP-2 and MMP-9 was determined semiquantitatively by densitometry. Gelatin zymography standards for enzymes and proenzymes of human MMP-2 and human MMP-9 (Chemicon International, Temecula, CA) were used.

Isolation of subcellular fractions

Cells were harvested and low-speed centrifuged, then the pellet was dispersed by vortexing in lysis buffer (50mM Tris-HCl (pH¹/₄8.0), 1% Triton X-100, 10% glycerol, 1mM EDTA, 250mM NaCl, 1mM dithiothreitol, 1mM phenylmethylsulfonylfluoride, 2mM sodium vanadate, 100mM sodium fluoride, 10 mg/ml aprotinin, 10 mg/ml leupeptin and 10 mg/ml pepstatin) for 10 min at 4 °C. Isolation of cytosol, nuclear and mitochondrial fractions was carried out by standard lab protocols exactly as described previously [26].

Western blot

Cells were washed with PBS, and directly lysed in lysis buffer. Cell lysates were adjusted to equal protein concentrations (NanoDrop Technologies, Inc., Wilmington, DE), resuspended in 2X sample loading buffer containing 4% SDS, 20% glycerol, 120mM Tris and bromophenol blue, and were boiled for 5 min. Protein samples were subjected to SDS-polyacrylamide gel electrophoresis. Proteins on the gel were transferred onto nitrocellulose membranes that were blocked with 50-50% Odyssey buffer and phosphate buffered saline (PBS) for 1 h at room temperature. Afterwards, the membranes were incubated with the indicated primary antibodies overnight at 4 °C. Primary antibody for GHRH-R was purchased from Abcam (ab28692, Abcam Inc., Cambridge, MA). E-cadherin, caveolin-1, β -catenin primary antibodies were purchased from Cell Signaling. NF- κ B and MMP-2 primary antibodies were purchased from Santa Cruz Biotechnology, Inc.. Alpha-tubulin primary antibody was obtained from Calbiochem. After being washed with PBS containing 0.1% Tween-20, the membranes were incubated with the appropriate secondary antibody. The immunoreactive bands were visualized with the Odyssey Infrared Imaging System (LI-COR Biosciences, Lincoln, Nebraska).

Wound migration assay

DBTRG-05, MDA-MB-468, and ES-2 cells (2×10^5) were seeded into six-well plates and grown to 100% confluency. After starvation of the cells, the confluent cells were carefully wounded with sterile polished pasteur pipette tips and any cellular debris were removed by washing with PBS. The wounded monolayers were then incubated in the presence of 1 μ M MIA-602 for 6 h and 24 h and digitally photographed. The distance between the wound edges was measured using Adobe Photoshop 6.0.

Migration assay

Cell migration assays were performed according to the manufacturer's protocol. The BD Falcon Cell Culture Insert System containing PET (polyethylene terephthalate) membranes with 8 μ m pores (BD Biosciences Discovery Labware Franklin Lakes, NJ) was utilized in the assay. DBTRG-05, MDA-MB-468, and ES-2 cells were harvested, after a 24 hour starving period, and resuspended into serum-free medium containing 1.0 μ M GHRH antagonist or the vehicle. The upper chamber of the insert was filled with 500 μ l of the cell and drug suspension (1×10^5 cells) and 1.5 ml of fibroblast-conditioned medium (FCM) was added to the lower chamber. FCM served as the chemoattractant. The conditioned medium was collected from NIH/3T3 cells grown in serum-free DMEM after 24 hours. The plate was incubated in a humidified environment at 37°C with 5% CO₂ for 24 hours. Cells were allowed to migrate or invade for 24 h. Cells that had not penetrated the filters were removed by scrubbing with cotton swabs. Chambers were fixed in 100% methanol for 10 min, stained in 0.5% crystal violet for 10 min, rinsed in PBS and examined under a bright-field microscope. Values for invasion and migration were obtained by counting five fields per membrane. Our results represent the average of three independent experiments performed over multiple days.

Data Analysis

Quantification of band density was performed using the Odyssey Infrared Imaging System (LI-COR Biosciences, Lincoln, Nebraska). Data shown in the figures are representative of at least three different experiments. The results are expressed as the mean \pm SEM and were statistically treated by following the Bonferroni's test for multiple comparisons after one- or two-way analysis of variance (ANOVA). The level of significance was set at $P < 0.05$.

Results

(for the study regarding Hsp 16.2)

Expression and intracellular localization of Hsp16.2 in different brain tumors by immunohistochemistry

Ninety-one samples of different brain tumors were evaluated in the present study (Table 1.): 5 schwannomas (grade 1), 6 pilocytic astrocytomas (grade 1), 6 meningothelial meningiomas (grade 1), 5 fibrous meningiomas (grade 1), 8 diffuse astrocytomas (grade 2), 5 oligodendrogliomas (grade 2), 6 ependymomas (grade 2), 5 atypical meningiomas (grade 2), 6 malignant meningiomas (grade 3), 5 anaplastic astrocytomas (grade 3), 5 anaplastic oligodendrogliomas (grade 3), 9 glioblastomas (grade 4), 5 giant cell glioblastomas (grade 4), 8 medulloblastomas (grade 4) and 7 PNETs (primitive neuroectodermal tumor) (grade 4) .

Table 1 - Immunohistochemical analysis of Hsp16.2 in 51 human brain tumors.

| Histological diagnosis | No. of cases | Tumor grade | Intracytoplasmic labeling | | | | Intranuclear labeling | | | |
|---------------------------|--------------|-------------|---------------------------|---|----|-----|-----------------------|---|----|-----|
| | | | - | + | ++ | +++ | - | + | ++ | +++ |
| Schwannoma | 5 | 1 | 5 | | | | | | | 5 |
| Pilocytic astrocytoma | 6 | 1 | 3 | 3 | | | | | | 6 |
| Meningothelial meningioma | 6 | 1 | 4 | 2 | | | | | | 6 |
| Fibrous meningioma | 5 | 1 | 2 | 3 | | | | | | 5 |
| Diffuse astrocytoma | 8 | 2 | 3 | 5 | | | | | | 8 |
| Oligodendroglioma | 5 | 2 | 1 | 4 | | | | | | 5 |
| Ependymoma | 6 | 2 | | 1 | 5 | | | | 1 | 5 |

| | | | | | | | | | | |
|------------------------------|---|---|--|---|---|---|--|--|--|---|
| Atypical meningioma | 5 | 2 | | 1 | 4 | | | | | 5 |
| Malignant meningioma | 6 | 3 | | | 6 | | | | | 6 |
| Anaplastic astrocytoma | 5 | 3 | | | 5 | | | | | 5 |
| Anaplastic oligodendroglioma | 5 | 3 | | | 5 | | | | | 5 |
| Glioblastoma | 9 | 4 | | | 2 | 7 | | | | 9 |
| Giant cell glioblastoma | 5 | 4 | | | | 5 | | | | 5 |
| Medulloblastoma | 8 | 4 | | | | 8 | | | | 8 |
| PNET | 7 | 4 | | | | 7 | | | | 7 |

Staining intensity: (+) mild, (++) moderate, (+++) strong

Hsp16.2 immunoreactivity was found both in the nucleus and in some cases in the cytoplasm in tumor tissues (Fig.1). Since intranuclear labeling was present in all tumor samples in large quantities, cytoplasmic Hsp16.2 immunoreactivity could be used for differential diagnostic purposes. Cytoplasmic labeling varied considerably among the different histological types and grades of tumors. Low grade tumors (grades 1-2) showed weak or no staining (+/-) in the cytoplasm (Fig.1. A, B). There was no detectable Hsp16.2 in the cytoplasm of the benign schwannoma (Fig.1.A) and one pilocytic- (Fig1.B) and two diffuse astrocytomas. The remaining low grade tumors stained weakly (Fig.1. C, E), excepting ependymomas (Fig.1.G) and atypical meningiomas, which stained moderately (++) .

Grade 3 tumors, including malignant meningiomas (Fig.1.F), anaplastic astrocytomas (Fig1.D) and oligodendrogliomas (Fig.1.H), displayed moderate cytoplasmic immunoreactivity for Hsp16.2. (++) . High grade tumors (grade 4) such as glioblastomas (Fig.1.I), medulloblastomas and PNETs (Fig.1.J) exhibited strong Hsp16.2 positivity in the cytoplasm. (+++)

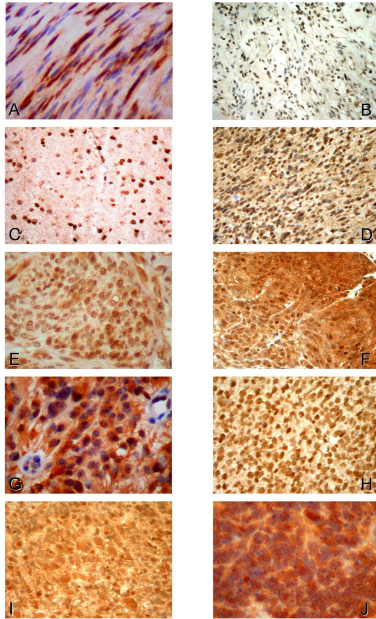


Figure 1 - Expression and intracellular distribution of Hsp16.2 in different human tumors of the nervous system.

Immunohistochemistry utilizing anti-Hsp16.2 primary antibody was performed on 91 brain tumor samples. **A.** Schwannoma. Intensive intranuclear Hsp16.2 immunoreactivity, whereas no immunoreactivity in the cytoplasm. **B.** Pilocytic astrocytoma. Strong intranuclear immunopositivity but no intracytoplasmic staining was detected. **C.** Grade 2 astrocytoma shows intensive intranuclear labeling as well as mild cytoplasmic staining. **D.** Grade 3 astrocytoma exhibits strong Hsp 16.2 positivity intranuclearly and moderate Hsp16.2 positivity in the cytoplasm. **E.** Grade 1 meningioma showing high expression of Hsp16.2 intranuclearly and mild expression in the cytoplasm. **F.** Grade 3 meningioma displayed strong intranuclear and moderate cytoplasmic staining for Hsp16.2. **G.** Grade 2 ependymoma with strong intranuclear and moderate cytoplasmic immunopositivity. **H.** Grade 3 oligodendroglioma exhibiting intensive intranuclear and moderate cytoplasmic immunoreactivity. **I.** Grade 4 glioblastoma showing strong Hsp16.2 positivity intranuclearly and intracytoplasmically alike. **J.** Grade 4 PNET with intensive staining in the nucleus as well as in the cytoplasm.

Table 2. shows the correlation between the cytoplasmic staining and the histological grades of different brain tumors.

Table 2 - Correlation of Hsp16.2 cytoplasmic expression and histological grade of brain cancer.

| Hsp16.2 expression | Grade 1 n (%) | Grade 2 n (%) | Grade 3 n (%) | Grade 4 n (%) | Total n (%) | P Value |
|--------------------|------------------|------------------|------------------|------------------|----------------|---------|
| - | 14 (63.6) | 4 (16.6) | | | 18 (19.8) | <0.01 |
| + | 8 (36.4) | 11(45.8) | | | 19 (20.8) | |
| ++ | | 9 (37.6) | 16 (100) | 2 (6.9) | 27 (29.7) | |
| +++ | | | | 27 (93.1) | 27 (29.7) | |
| Total | 22 (100) | 24 (100) | 16 (100) | 29 (100) | 91 (100) | |

Staining intensity: (+) mild, (++) moderate, (+++) strong

There was no cytoplasmic expression in 63.6% and mild expression in 36.4% of Grade 1 cancers. 16.6 % showed no, 45.8% exhibited mild and 37.6% of the samples displayed moderate staining in Grade 2 cancers. All (100%) Grade 3 cancers demonstrated moderate staining. Only 6.9% of Grade 4 tumor samples revealed moderate immunoreactivity, while 93.1% proved to be intensively stained. These results clearly demonstrate that the Hsp16.2 staining of the cytoplasm is directly correlated with the histological grade of the brain tumors.

Detection of Hsp16.2 expression by Western-blot

After subcellular fractionation, the expression of Hsp16.2 was determined from both the cytosolic (Fig. 2.) and the nuclear fraction by immunoblotting. Thirty samples were studied including three from normal brain tissue, and three samples from nine different types of brain tumors. The intranuclear expression of Hsp16.2 was approximately the same level in the different samples (data not shown). Three samples from different parts of the brain were tumor-free, serving as a negative control for the experiment, which contained a minimal amount of nuclear and cytoplasmic Hsp16.2 (lane 1). Low cytoplasmic expressions of the protein were visible in grade 1 meningiomas, pilocytic astrocytomas (lane 2, 3). The expression was stronger in the Grade 2 diffuse astrocytomas and ependymomas (lane 4, 5). Higher cytoplasmic expressions of Hsp16.2 were observed in grade 3 tumors such as anaplastic astrocytomas and malignant meningiomas (6, 7). The strongest bands appeared in the cytoplasmic samples of medulloblastomas, PNETs and glioblastomas (8-10). In conclusion, the observed Hsp16.2 labeling correlated with the results gained by the immunohistochemistry method.

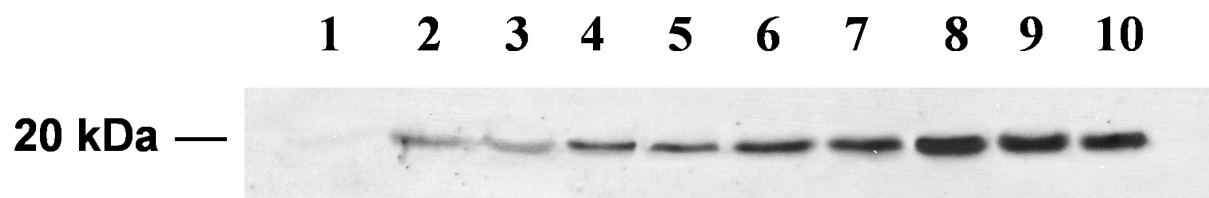


Figure 2 - Cytoplasmic expression of Hsp16.2 in different human brain tumors. Endogenous cytoplasmic expression levels of Hsp16.2 were assessed by Western blotting utilizing a custom made polyclonal anti-Hsp16.2 primary antibody. 30 samples were used including three from normal brain tissue and 18 samples from nine different types of brain cancer, two samples from each type. The subcellular fractionation was confirmed by probing with antibodies recognizing nuclear H3 histone, cytoplasmic actin and equal loading was confirmed by a second incubation with anti-GAPDH antibody (data not shown). 1: normal

brain, 2: Pilocytic astrocytoma (Grade 1), 3: Meningothelial meningioma (Grade1) 4: Diffuse astrocytoma (Grade 2), 5: Ependymoma (Grade 2), 6: Malignant meningioma (Grade 3), 7: Anaplastic astrocytoma (Grade 3), 8: Medulloblastoma (Grade 4), 9: Giant cell glioblastoma (Grade 4), 10: PNET (Grade 4)

(for experiments regarding the mechanism of action of GHRH antagonists)

The presence of pituitary GHRH receptor and its splice variant, SV1 on DBTRG-05 and U-87MG glioblastoma cell lines

We investigated whether pGHRH-R and SV1 are present on both cell lines using Western blot method. SV1 of GHRH-R has the greatest structural similarity to the pGHRH-R and is considered the main truncated splice variant [28]. For the detection, we used polyclonal antiserum against the polypeptide segment, found in both pGHRH and SV1 receptors. Both types of receptors were detected on the two glioblastoma cell lines, pGHRH-R at 60 kDa and SV1 at 39.5 kDa. pGHRH-R was expressed at a significantly higher level than SV1 in both cell lines. (Fig. 1) Our results correspond to earlier findings on pGHRH-R and SV1 detection [21; 28]. NIH/3T3 cells were used as a negative control since they express neither pGHRH nor SV1 receptors [19; 29].

Figure 1

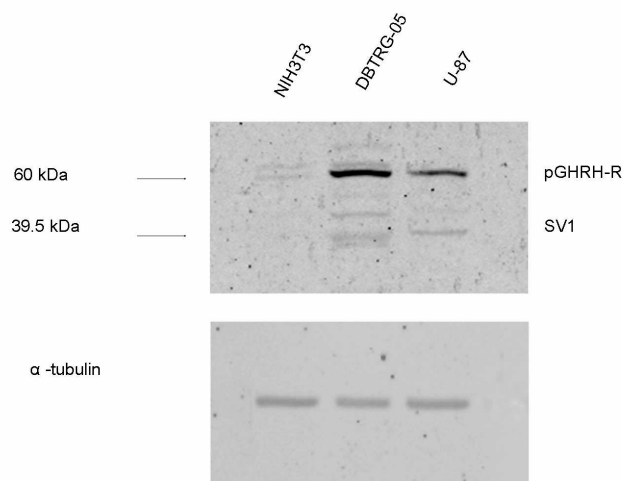


FIGURE 1 – Western blot analysis of pGHRH-R and SV1, with α -tubulin as control in samples from NIH/3T3, DBTRG-05 and U-87MG cell lines. All immunoreactive signals were detected with a commercial polyclonal antiserum against a polypeptide segment that is present in both SV1 and pGHRH receptors. The molecular masses are shown.

The inhibitory effect of GHRH antagonists JMR-132 and MIA-602 on glioblastoma cell viability

DBTRG-05 and U-87MG cancer cell lines, were exposed to GHRH antagonists JMR-132 and MIA-602 at 0.1, 1, 5 and 10 μ M concentrations for 48 hours. The untreated cells served as negative controls. The GHRH antagonists inhibited cell proliferation in all concentrations. The concentration, at which cellular growth was inhibited by 30% (IC 30), was 1 μ M. Consequently, we used this concentration in our experiments. After treatment with 1 μ M JMR-132 and MIA-602 the cell viability decreased significantly, by 32% and 34%, respectively in DBTRG-05 cells and by 31 % and 32%, respectively in U-87MG cells (Fig. 2a, b). In contrast, GHRH(1-29)NH₂ at a concentration of 1 μ M stimulated the proliferation of DBTRG-05 and U-87MG cells (Fig. 2c). GHRH antagonists at the same concentration inhibited cell proliferation and abolished the effect of exogenous GHRH(1-29)NH₂ (Fig. 2c).

Figure 2

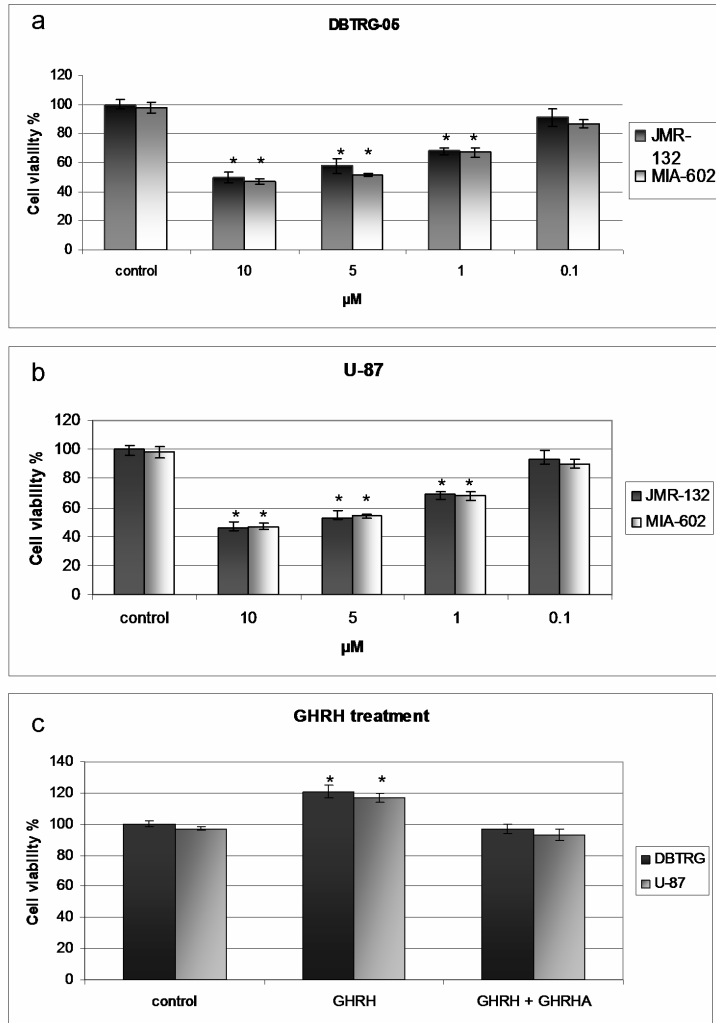


FIGURE 2 – The inhibitory effect of GHRH antagonists, JMR-132 and MIA-602 at different concentrations on (a) DBTRG-05 and (b) U-87MG in different concentrations. (c) The effect (c) of GHRH(1-29)NH₂ (GHRH) alone and in combination with the GHRH antagonist (GHRHA), MIA-602 at a concentration of 1 μM, on DBTRG-05 and U-87MG cell lines. The combination of GHRH(1-29)NH₂ with JMR-132 gave similar results. (Data not shown) Cell viabilities were measured by an MTT (methylthiazolyldiphenyl-tetrazolium bromide) assay

and were expressed as percentage of untreated cells. The results are mean \pm SEM of three independent experiments performed at least in quadruplicate. *P< 0.05.

The effect of GHRH antagonists JMR-132 and MIA-602 on cell signaling pathways in glioblastomas

In order to examine whether GHRH antagonists JMR-132 and MIA-602 can diminish the levels of anti-apoptotic proteins, levels of phospho-AKT, phospho-GSK3 β and phospho-ERK1/2 were determined at 0, 5, 10, and 30 minutes following exposure of both glioblastoma cell lines to 1 μ M of JMR-132, MIA-602 and GHRH(1-29)NH₂. Western blots were used to assess the results. Treatment with the GHRH antagonists resulted in a significant decrease in the expression of p-AKT and pGSK3 β at 5 minutes, an even greater decrease at 10 minutes, but an increase to their initial, "0" minute, level at 30 minutes (Fig. 3a, b). Following treatment with the GHRH antagonists, p-ERK1/2 expression levels also fell significantly at 5 minutes, remained low at 10 minutes then rose at 30 minutes (Fig. 3c). The agonist-treated cells showed an elevation in the levels of p-AKT, p-GSK3 β and p-ERK1/2 at 5 minutes, a greater elevation at 10 minutes, and eventually returned to their original phosphorylated state at 30 minutes (Fig. 3a, b, c) The intensity of pro-apoptotic protein phospho-p38 expression was determined at "0" time point, which served as a control, and after 24 hours of treatment. Cells treated with GHRH antagonists displayed a major activation of p38 MAP kinase phosphorylation (Fig. 3d). A slight increase of phospho-p38 was demonstrated in GHRH(1-29)NH₂ treated cells (Fig. 3d). Similar results were obtained in the DBTRG-05 and U-87MG cell lines (data not shown). MIA-602 caused a slightly greater change in the levels of the above-mentioned proteins, but the difference between the two GHRH antagonists was not significant.

Figure 3

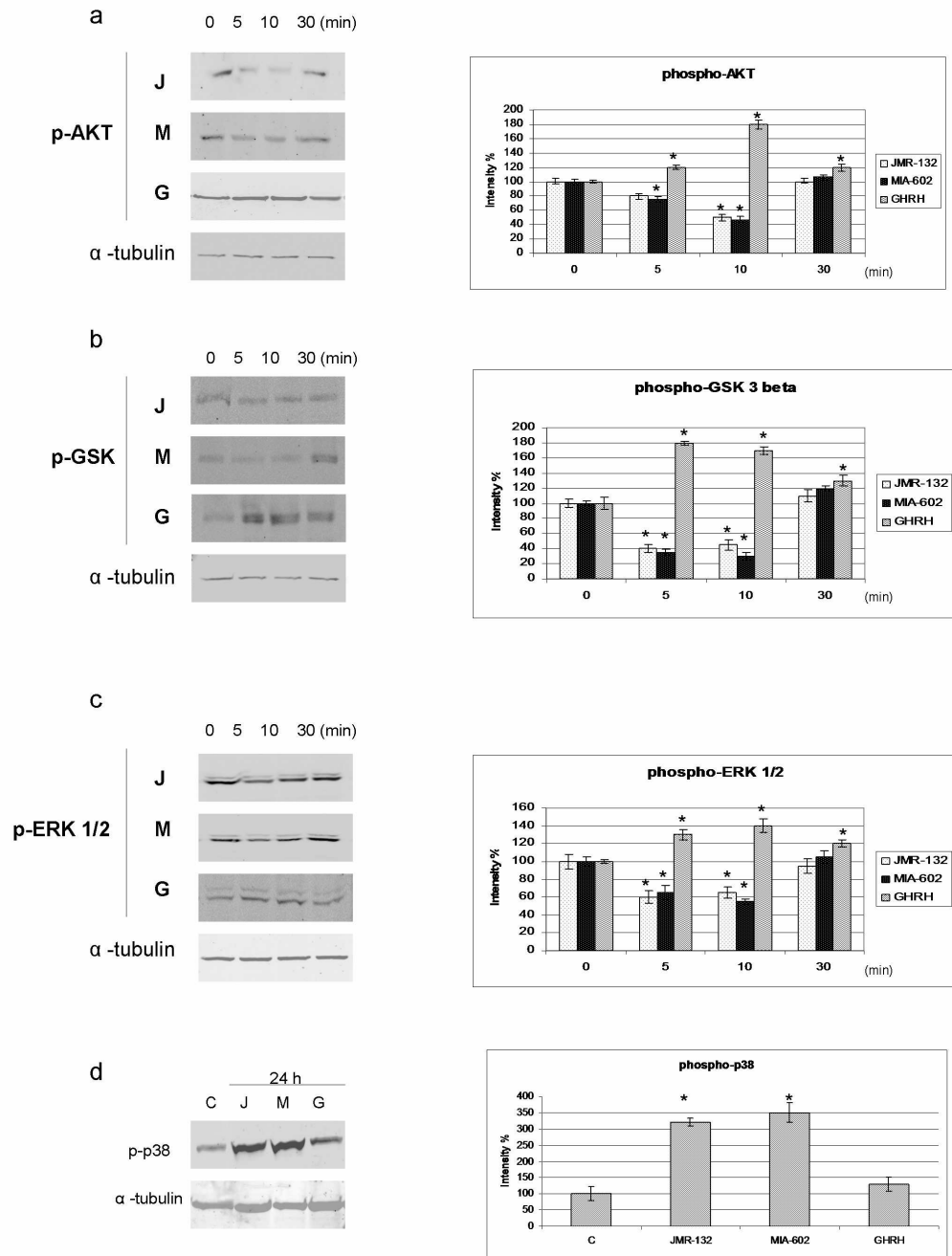


FIGURE 3 – The effect of GHRH antagonists, JMR-132 (J) and MIA-602 (M) and GHRH(1-29)NH₂ (G) on the activation of (a) Akt (b) GSK3 β (c) ERK 1/2 and (d) p38 MAP kinases in samples from DBTRG-05 cells at 0, 5, 10 and 30 minutes as demonstrated by immunoblotting utilizing phosphorylation specific primary antibodies against the given kinase. Similar results were obtained when the experiments were repeated with samples from U-

87MG cells (data not shown). α -tubulin immunoreactivity was used to show even loading. Representative blots of three independent experiments are presented. * $P < 0.05$.

The effect of GHRH antagonists JMR-132 and MIA-602 on the key executioners of apoptosis

DBTRG-05 and U-87 were treated with JMR-132 and MIA-602 at 1 μ M concentration for 6 and 24 hours. Western blot analysis of the samples showed the appearance of cleaved caspase-3 after 6 hours of treatment, followed by its intense expression after 24 hours of treatment (Fig. 4b). A similar result was found when changes in the cleaved PARP levels were examined. Although the presence of cleaved PARP was examined at an additional time point (at 4 hours), cleaved PARP could only be detected after 6 hours and 24 hours of treatment, with higher levels observed at the later time point (Figure 4a). Treatment with 10 μ M did not result in cleavage of PARP or of caspase-3 (Fig. 4a, b). No major differences between the effects of the two GHRH antagonists on protein cleavage could be identified. Western blot analyses of both glioblastoma cell lines provided similar results.

Figure 4

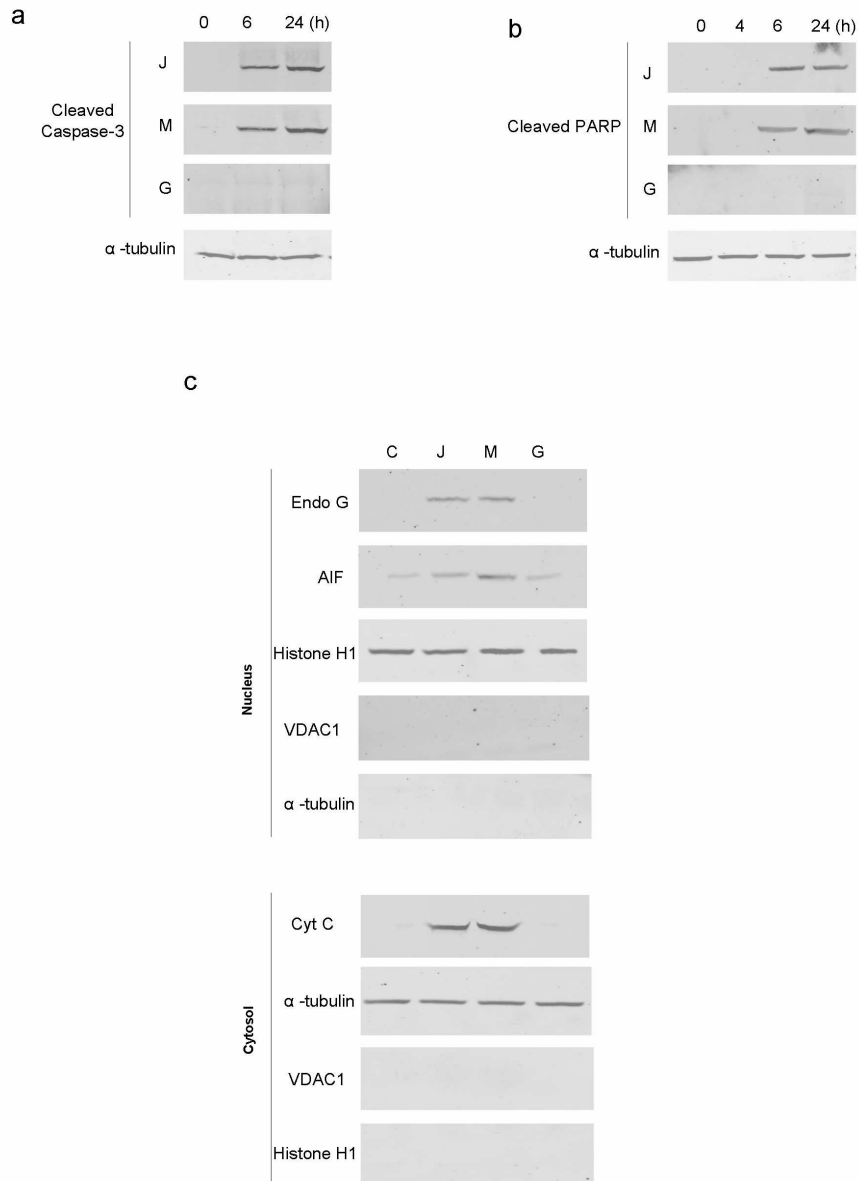


FIGURE 4 – The effect of GHRH antagonists, JMR-132 (J) and MIA-602 (M) and GHRH(1-29)NH₂ (G) on the expression of cleaved (a) PARP and (b) caspase-3 at (a) 0, 6 and 24 hours and (b) 0, 4, 6 and 24 hours in samples from DBTRG-05 cells displayed by Western blot using appropriate primary antibodies. Similar results were obtained when the experiments were repeated with U-87MG cells (data not shown). α -tubulin immunoreactivity was used to

show even loading. Representative blots of three independent experiments are presented. (c) Immuno-blot analysis of the pro-apoptotic mitochondrial proteins Endo G, AIF and cyt c detected in the nuclear and cytosolic fractions of the DBTRG-05 cells following treatment with GHRH antagonists, JMR-132 (J) and MIA-602 (M) and GHRH(1-29)NH₂ (G). Cells not treated served as controls (C). Similar results were gained when the experiments were repeated with samples from U-87MG cells (data not shown). Loading was checked by specific markers, the mitochondrial marker VDAC1/porin (VDAC1), cytosol marker α -tubulin and the nuclear marker Histon H1 (Histon H1). Representative blots of three independent experiments are presented.

The effect of GHRH antagonists JMR-132 and MIA-602 on the release of pro-apoptotic proteins

Following a variety of apoptotic stimuli and the collapse of mitochondrial membrane potential, pro-apoptotic proteins; AIF, Endo G and cyt c are released from the mitochondria. Subsequent to treatment for 24 hours with GHRH(1-29)NH₂ and GHRH antagonists at 1 μ M concentration, the localization of these proteins was detected by Western blot method. Treatment with GHRH(1-29)NH₂ did not change the intracellular localization of the above-mentioned proteins (Fig. 4). After treatment with 1 μ M of GHRH antagonists JMR-132 and MIA-602, the release of cyt c from the mitochondria to the cytosol as well as the nuclear translocation of AIF and Endo G was observed (Fig. 4c).

The effect of GHRH antagonists JMR-132 and MIA-602 on the mitochondrial membrane potential

The membrane potential sensitive dye, JC-1 and fluorescence microscopy were used to visualize the depolarization of the mitochondria. Red fluorescence (590 nm) can be seen when mitochondria are intact, while green fluorescence (530 nm) becomes visible when the mitochondrial membrane potential is decreased. Green fluorescence occurs when cells are undergoing apoptosis. A 6 hour and 24 hour treatment with 1 μ M JMR-132 (Fig 5 b,c) and MIA-602 (Fig. 5 e,f), completely abolished the red fluorescence at 24 h, and the mitochondria were visible as intense green spots. Untreated cells (Fig. 5 a) as well as those treated with GHRH(1-29)NH₂ (Fig. 5d) displayed an even red fluorescence indicating an unchanged mitochondrial membrane potential.

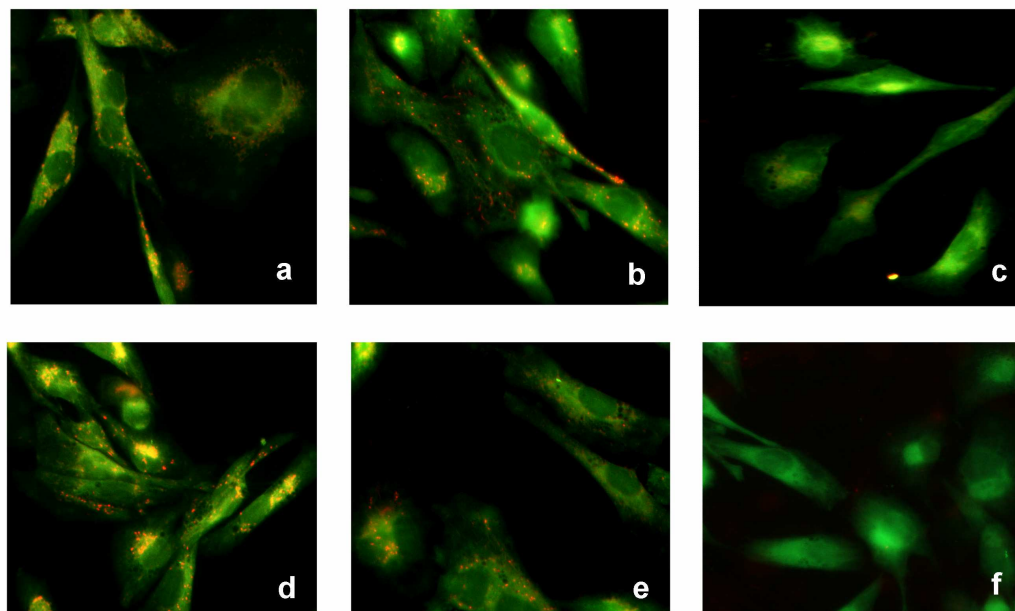
Figure 5

FIGURE 5 - Effect of treatment with JMR-132, MIA-602 or GHRH(1-29)NH₂ on the mitochondrial membrane potential of DBTRG-05 cells. Green and red fluorescence images were merged and used to demonstrate the integrity of the mitochondrial membrane potential in JC-1 loaded control (a) DBTRG cells. The cells were treated with 1 μ M JMR-132 (6h: *b*, 24h: *c*) and MIA-602 (6h: *e*, 24h: *f*) for 6 and 24 hours to induce mitochondrial membrane damage before washing, loading and imaging. The 24 hour treatment (*d*) with GHRH(1-29)NH₂ had no effect on mitochondrial membrane visualized by JC-1. Representative images of three independent experiments are presented.

The effect of GHRH antagonist MIA-602 on the growth of DBTRG-05 human glioblastoma, in vivo

Treatment with GHRH antagonist MIA-602 at the dose of 5 µg/day was initiated after the tumors reached a volume of approximately 70 mm³ and continued for 35 days. A significant tumor growth reduction at the end of the second week of treatment was observed in the treated group, but the greatest suppression ($p < 0.001$) in the tumor volume compared with controls was found from weeks 2 to 5 of therapy (Fig. 6). After treatment with MIA-602, the tumor growth reduction rate ($p < 0.001$ versus controls) was 68.98 % and the treatment significantly ($P < 0.05$) extended tumor doubling time as compared with controls (Table I).

Figure 6

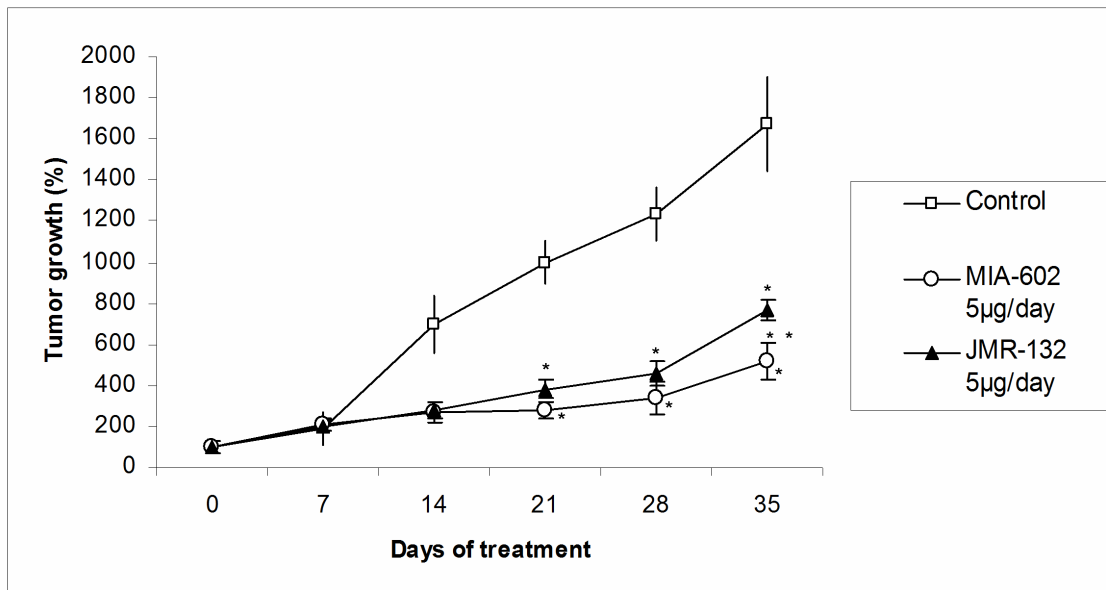


FIGURE 6 - Effect of treatment with GHRH antagonists, MIA-602 and JMR-132, given s.c. at a dose of $5\mu\text{g/day}$ on the tumor growth of DBTRG-05 human glioblastoma cancer xenografted s.c. into nude mice. Vertical bars indicate SE. *, $P < 0.001$ vs. control; **, $P < 0.05$ MIA-602 vs. JMR-132.

Table 1. Effect of therapy with GHRH antagonists MIA-602 and JMR-132 on the growth of DBTRG-05 human glioblastoma cancer xenografted into nude mice

| Treatment | Initial tumor volume, mm ³ | Final tumor volume, mm ³ (%inhibition) | Tumor weight, mg | Tumor doubling time, days | Body weight on day 34, g |
|-----------------|---------------------------------------|---|------------------|---------------------------|--------------------------|
| Control | 74.2 ±5.2 | 1673±232 | 1780.3±32 | 7.2±0.4 | 25.3±1.2 |
| MIA-602 5µg/day | 72.3±5.8 | 519.4±63 (69)* | 902±132* | 11±0.3** | 24.2±1.3 |
| JMR-132 5µg/day | 69.4±4.5 | 764±42 (55)* | 1098±97* | 9.8±0.3** | 24.9±1.7 |

* P < 0.05, **P<0.01 vs. control.

(for experiments regarding the reduction of invasion- and metastasis- potential of cancer cells by GHRH antagonists)

The presence of pGHRH-R and its splice variant, SV1 on DBTRG-05, MDA-MB-468 and ES-2 cell lines

We investigated whether pGHRH-R and SV1 are present on all three cell lines using Western blot method. SV1 of GHRH-R has the greatest structural similarity to the pGHRH-R and is considered the main truncated splice variant [28]. For the detection, we used polyclonal antiserum against the polypeptide segment, found in both pGHRH and SV1 receptors. Both types of receptors were detected on all three cancer cell lines, pGHRH-R at 60 kDa and SV1 at 39.5 kDa, although both receptors were expressed at the highest level in MDA-MB-468 cells, and at a lesser extent in the other two cell lines. pGHRH-R was expressed at a significantly higher level than SV1 in all three cell lines. (Fig. 1) Our results correspond to earlier findings on pGHRH-R and SV1 detection [21; 30]. NIH/3T3 cells were used as a negative control since they express neither pGHRH nor SV1 receptors [29].

Figure 1

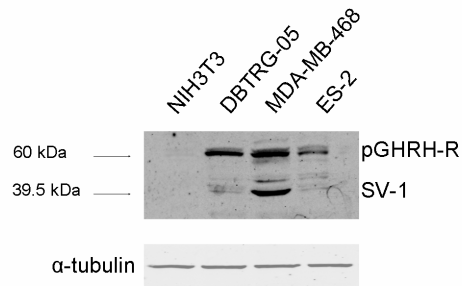


Fig. 1. Western blot analysis of pGHRH-R and SV1, with α -tubulin as control in samples from NIH/3T3, DBTRG-05, MDA-MB-468 and ES-2 cell lines. All immunoreactive signals were detected with a commercial polyclonal antiserum against a polypeptide segment that is present in both SV1 and pGHRH receptors. The molecular masses are shown

The inhibitory effect of GHRH antagonist MIA-602 on cell proliferation

DBTRG-05, MDA-MB-468 and ES-2 cancer cell lines, were exposed to GHRH antagonist, MIA-602 at 0.1, 1, 5 and 10 μM concentrations for 48 hours. The untreated cells served as negative controls. MIA-602 inhibited cell proliferation at all concentrations. Since the concentration, at which cellular growth was inhibited by 30% (IC 30), was 1 μM , we used this concentration in our experiments further on in our study. After treatment with 1 μM MIA-602 the cell viabilities decreased significantly, by 34% in DBTRG-05 cells, by 30 % in MDA-MB-468 cells and by 32% in ES-2 cells (Fig. 2).

Figure 2

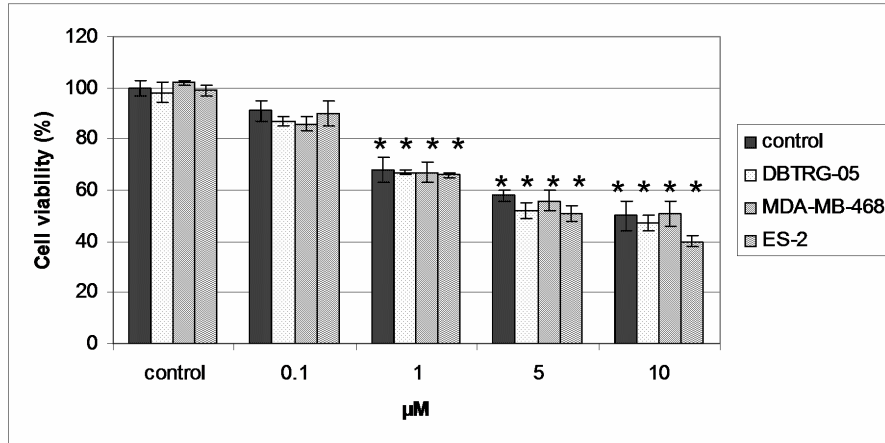


Fig. 2. The inhibitory effect of GHRH antagonist MIA-602 on cell viability of DBTRG-05, MDA-MB-468 and ES-2 in different concentrations. Cell viabilities were measured by an methylthiazolyldiphenyl-tetrazolium bromide MTT assay and were expressed as percentage of untreated cells of three independent experiments performed at least in quadruplicate. Vertical bars represent SEM. *P< 0.05.

Inhibitory effects of MIA-602 on cancer cell adhesion

The increased cell adhesion to the extracellular matrix (ECM) is considered an important step in the acquisition of metastatic properties in cancer cells. Cell adhesion assays were used to determine the ability of the tumor cells to bind ECM components. All three cell lines were treated with the GHRH antagonist then added to fibronectin precoated plates and allowed to adhere for 30, 60 and 90 minutes. Compared to the controls, all three cells showed significantly decreased attachment to fibronectin. At 90 minutes the adhesion ratio of DBTRG-05, MDA-MB-468 and ES-2 decreased significantly, by 30%, 34 % and 54% respectively (Fig. 3a). Following the treatment, when the tumor cells were added to matrigel precoated plates, similar results were observed. The adhesion ratio to matrigel diminished in DBTRG-05 cells by 34 %, in MDA-MD-468 cells by 31% and in ES-2 cells by 51% (Fig. 3b).

Figure 3

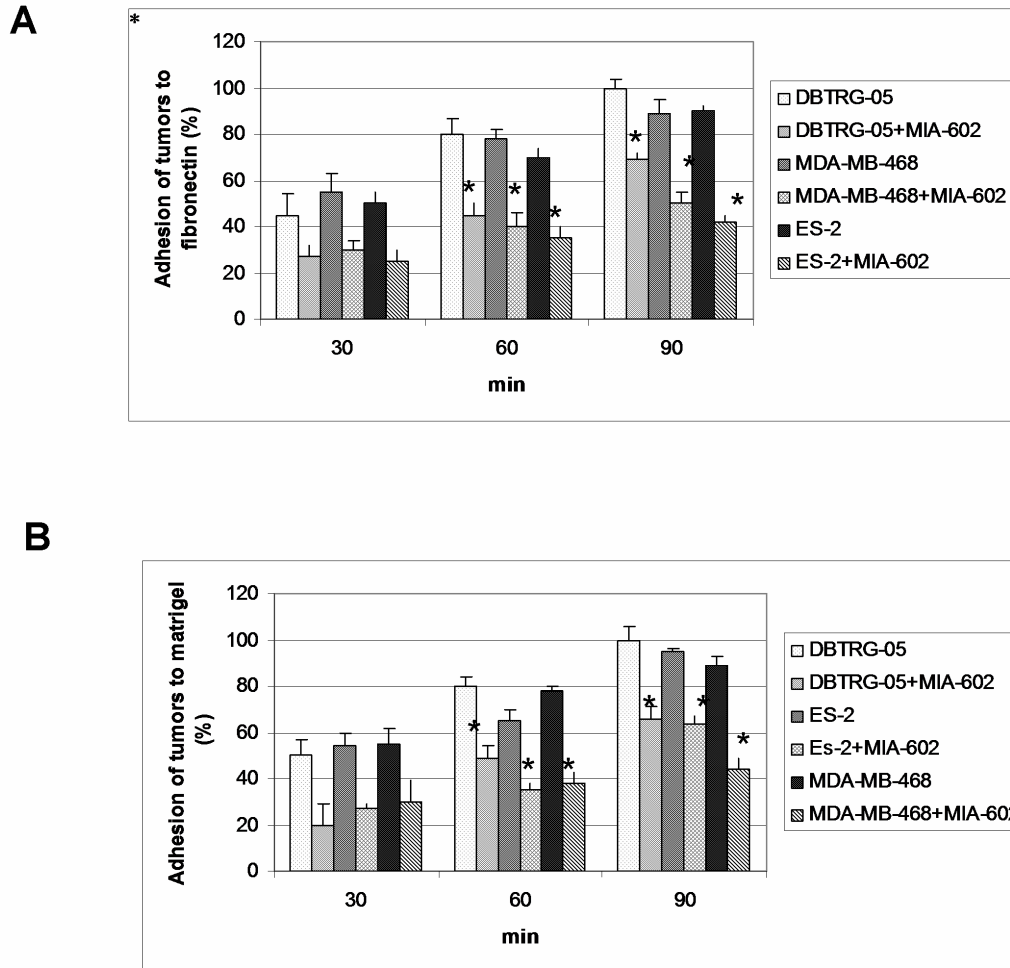


Fig. 3. The effect of GHRH antagonist MIA-602 on the adhesion of DBTRG-05, MDA-MB-468 and ES-2. Cells were incubated with or without 1 μ M MIA-602 and seeded onto 96-well plates precoated with (A) fibronectin or (B) matrigel. The remaining cells per well were measured after 30, 60 and 90 minutes. Data were representative of three separate experiments. Vertical bars represent SEM. *P < 0.05.

Inhibition of tumor cell invasion by MIA-602

A major issue of metastasis development is the invasion of tumor cells into surrounding tissues. Invasion chambers with matrigel-coated membranes were used to investigate the invasive properties of untreated (control) and GHRH antagonist treated cells. The average invasion rate of all three cancer cell lines (DBTRG-05, MDA-MB-468 and ES-2) decreased significantly after 24 hours of exposure to MIA-602 compared to untreated cells (Fig. 4). ES-2 cells showed the greatest reduction in their invasion rate following treatment, compared to the other two cell lines.

Figure 4

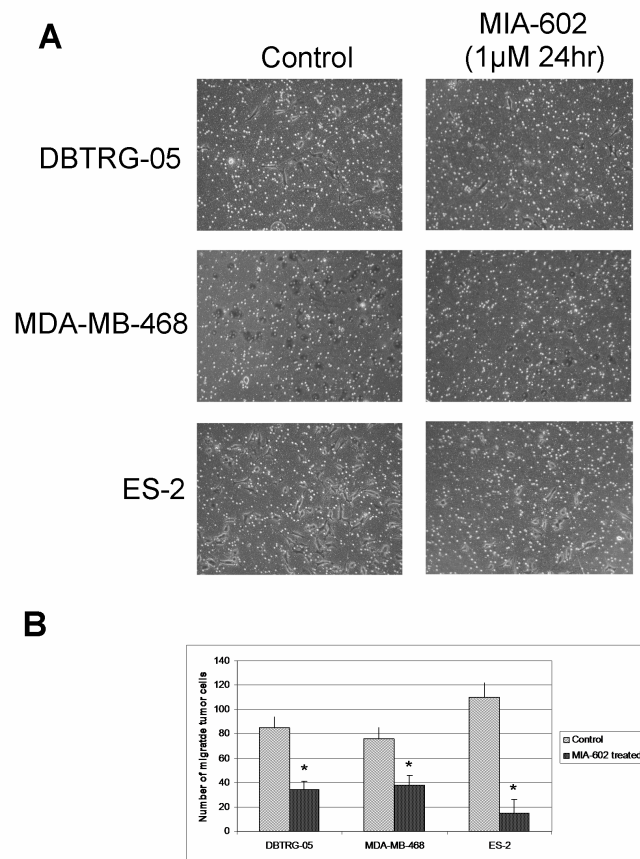


Fig. 4. The effect of GHRH antagonist MIA-602 on the invasion of DBTRG-05, MDA-MB-468 and ES-2 in vitro. (A) Photomicrographs show the invasion of the cells through the layer

of membrane and images were taken under 40x magnification. (B) Migration of cells through 8 μm Matrigel-coated polycarbonate pores was determined by the Boyden chamber model. Cells not exposed to MIA-602 were used as a control. Vertical bars represent SEM. * $P < 0.05$.

Inhibition of cell motility by MIA-602

Another measure of the metastatic potential of cancer cells is their increased motility. In order to examine, whether exposure to GHRH antagonist, MIA-602 affected the motile ability of the cells, we performed wound-healing assays. Wound closure was examined at 12 and 24 hours following treatment. The control cells migrated into the wound area by 24 hours to an extent that the wound edges were undistinguishable (Fig. 5a). However, cells, from all three cell lines, treated with the GHRH antagonist, displayed significantly slower wound closure at both time points, never completely closing the wound area (Fig. 5b). The motility of ES-2 cells was inhibited most by the GHRH antagonist, compared to the other two cell lines.

Figure 5

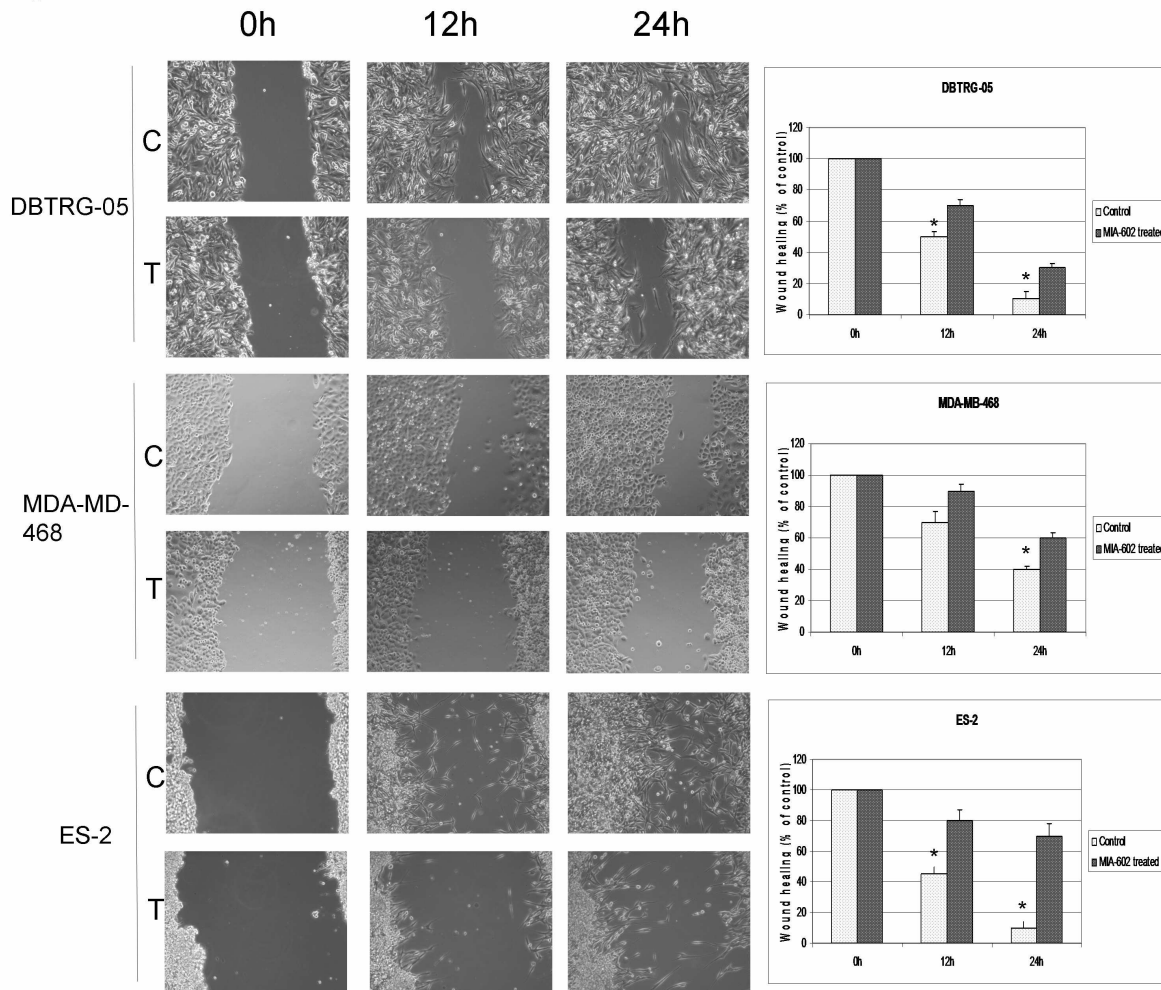


Fig. 5. The effect of GHRH antagonist MIA-602 on the cell motility of DBTRG-05, MDA-MB-468 and ES-2 demonstrated by wound-healing assays. Confluent cells cultured in six-well dishes were wounded with a sterile pipette tip and then incubated with or without 1 μ M MIA-602 for 0 h, 12 h and 24 h (C: control; T: treated). Photographs were taken with inverted microscope (Olympus CKX41) under 40x magnification and measurements were made with Adobe photoshop 6.0. Representative monolayer images are shown. Vertical bars represent SEM. *P < 0.05.

The effect of MIA-602 on the expression of adhesion, proliferation and invasion-associated molecules

We used immunoblotting to determine the expression of cell adhesion junction proteins (1), caveolin-1, E-cadherin and β -catenin following 6, 24 and 48 hours of MIA-602 treatment. Following 6 hours of treatment the levels of caveolin-1 and E-cadherin were significantly elevated and steadily rose, peaking at 24 hours in all three cancer cell lines (DBTRG-05, MDA-MB-468 and ES-2) (Fig. 6 a). On the other hand, β -catenin levels were dramatically reduced after MIA-602 treatment, reaching their lowest level at 24 hours (Fig. 6b). The expression of NF- κ B, a protein involved in the regulation of cellular survival, proliferation and carcinogenesis [31], was examined in the cell, cytosol and nuclear lysate of the three cancer cells after exposure to MIA-602. The GHRH antagonist treated cells showed decreased NF- κ B nuclear translocation and increased cytosolic expression, which indicates the potent inhibition of NF- κ B activation by MIA-602. One of the important downstream effectors of NF- κ B, MMP-2, [31; 32] plays a pivotal role in tumor invasion [33]. Using Western blot analysis, we detected the significant reduction of MMP-2 expression in MIA-602 treated cells (Fig. 6c). Results were similar in all three cell lines.

Figure 6

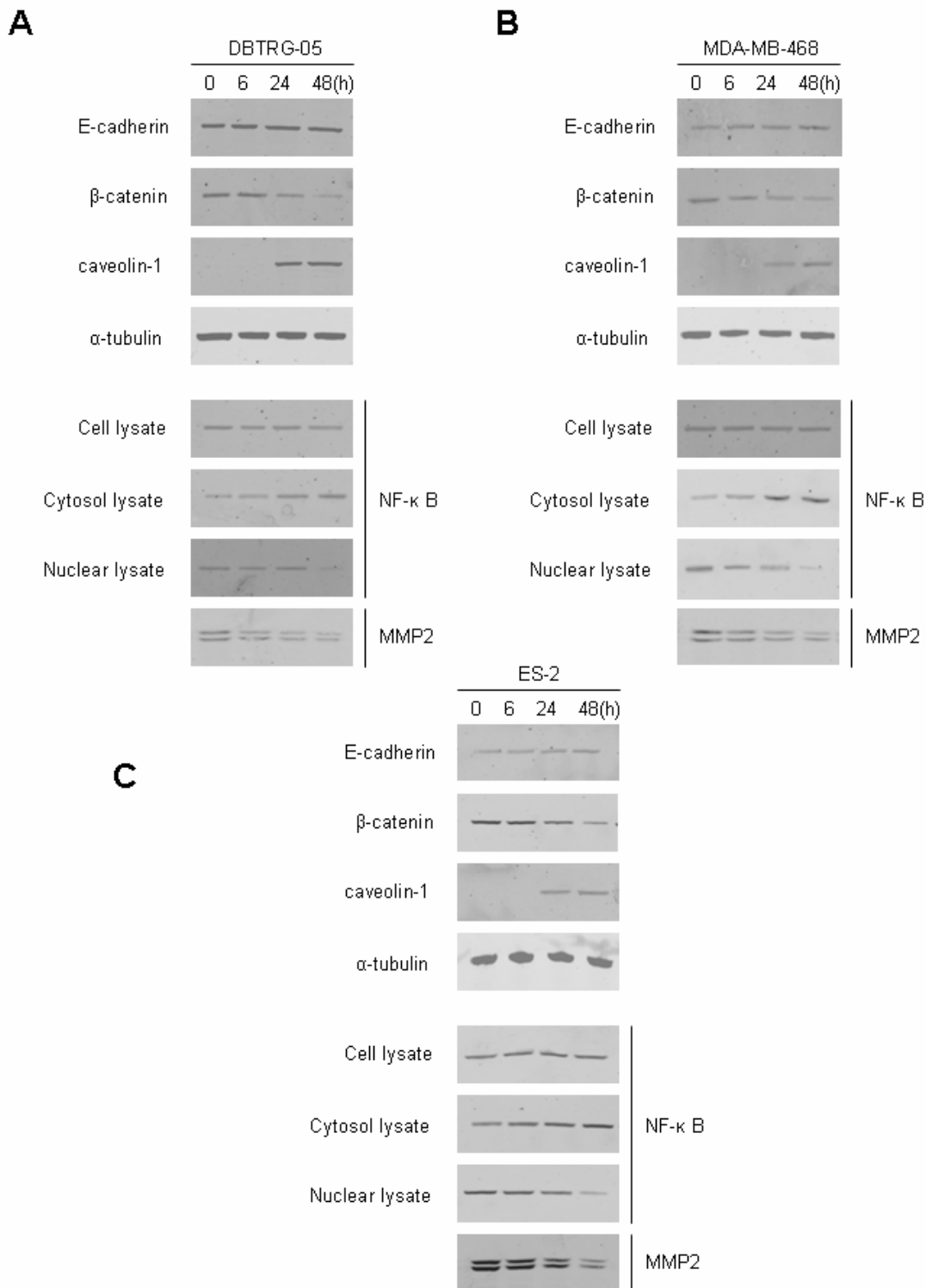


Fig. 6. The effect of GHRH antagonist MIA-602 on the activation of E-cadherin, caveolin-1 and inhibition of β -catenin, NF- κ B and MMP-2 activity on (A) DBTRG-05 (B) MDA-MB-468 and (C) ES-2 cell lines. The cells were collected at the indicated time points after being treated with 1 μ M MIA-602 and were analyzed by Western blot. The protein levels of NF- κ B

were analyzed in whole lysates, cytosol and nucleus by immunoblot to confirm the translocation. α -tubulin immunoreactivity was used to show even loading. Representative blots of three independent experiments are presented.

The inhibitory effect of MIA-602 on MMP-2 and MMP-9 expression

MMP-2 and MMP-9 are extracellular metalloproteinases which influence cell motility and invasion and are often upregulated in cancers [34]. The activity of these two matrix-metalloproteinases was investigated using gelatin zymography. Cells were treated with MIA-602 for 6, 12, 24 and 48 hours, then their supernatants were collected and the MMP activity measured. A gradual decrease in the activities of both MMP-2 and MMP-9 was observed from the first time point (6 hours), and was the lowest after 48 hours of treatment in all three cell lines (DBTRG-05, MDA-MB-468 and ES-2) indicating the potent inhibitory effect of MIA-602 (Fig. 7)

Figure 7

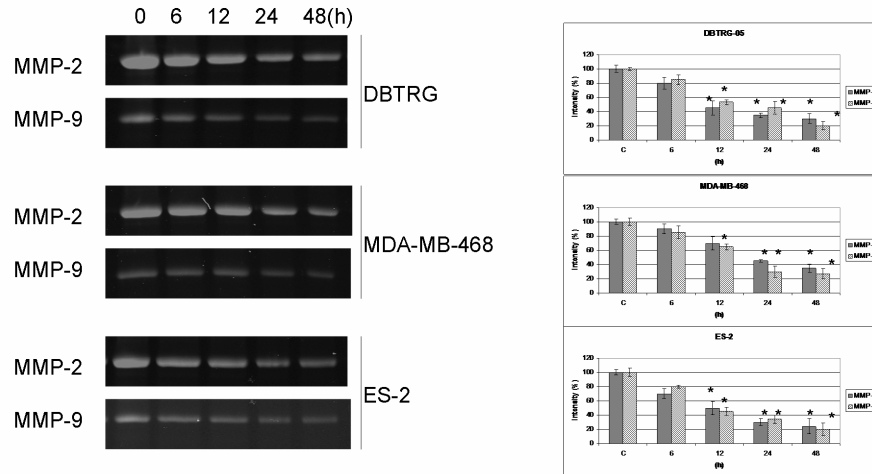


Fig. 7. The effect of GHRH antagonist MIA-602 on the enzymatic activities of MMP-2 and MMP-9 in (A) DBTRG-05 (B) MDA-MB-468 and (C) ES-2 cell lines. The activities of MMPs were determined by gelatinase zymography after exposure to 1 μ M MIA-602 with cell supernatants at the indicated time points. The densitometric analysis of MMPs is shown. Each bar represents mean \pm SEM from three independent experiments. *P < 0.05.

Discussion

Most malignant neoplasms in the brain already carry a dismal prognosis when they are diagnosed. Therefore, the treatment of human brain tumors possesses a continuous challenge for oncological research. Although several brain tumor markers have been investigated as possible prognostic factors, further research is needed to reveal the complex mechanism of tumor genesis, thus helping to discover the most appropriate tumor markers for prognosticating the neoplasm.

A number of recent studies have been concerned with the possible role of small heat shock proteins in the progression of brain tumors. Small stress proteins are a group of heat shock proteins that share an evolutionary conserved C-terminal region, called the alpha-crystallin domain, and whose molecular weight ranges between 15 and 43 kDas[7; 9; 11]. They are known to play a part in cell differentiation and in counteracting apoptosis [35]. Due to the anti-apoptotic activity of sHsps, tumor cells expressing the protein highly may become increasingly resistant to chemo- or radiotherapy [7; 36].

Aoyama et al. reported increased expression of alphaB-crystallin in human glial tumors such as astrocytomas and glioblastoma multiforme [37]. Astrocytic neoplasms were examined for Hsp27 immunoreactivity also. While normal astrocytes showed no Hsp27 immunoreactivity, low Hsp27 expression was found in benign astrocytomas and elevated levels of Hsp27 found in poorly differentiated tumors. There are data indicating the direct correlation between Hsp27 expression and the histologic grade of astrocytic tumors [38]. The prognostic significance of Hsp27, Hsp 70, and Hsp90 in medulloblastomas was examined with equivocally positive results [39].

Previously, we reported the existence of a novel small stress protein, sHsp16.2 and its high levels of expression in neuroectodermal cancers [26]. This finding turned our attention to examining sHsp16.2 expression in brain tumors differing in their grade and type. Since all ninety-one tumors were labeled equally intra-nuclearly, and they varied in their cytoplasmic labeling, it became apparent that the various tumors differed in the distribution and density of sHsp16.2 in the cell cytoplasm. In accordance with earlier studies, astrocytomas (grade 1-2) as well as other benign brain tumors, such as meningotheial meningeoma, and oligodendroglioma (grade 1-2) exhibited low expression (+) of Hsp16.2. In fact, certain benign brain tumors, like schwannoma and fibrous meningeoma showed no immunoreactivity at all. However, the increase of anaplasia in the tumor cells resulted in moderate (++)

expression (atypical meningioma, malignant meningioma, anaplastic astrocytoma, anaplastic oligodendroglioma) and high (++++) expression (glioblastoma, medulloblastoma, PNET) of the protein. Thus, it became evident that there is a direct correlation between the intensity of the staining and the histological grade of the brain tumor. Western blot analysis of thirty tumor samples gave similar results. It was observed, that no Hsp16.2 was found in normal brain tissue, while high Hsp16.2 labeling was observed in samples from medulloblastoma and glioblastoma. The observation that low levels were seen in Grade 1 meningiomas, pilocytic astrocytomas, moderate levels in grade 2 diffuse astrocytomas and ependymoma, stronger in grade 3 anaplastic astrocytomas and malignant melanoma, and elevated levels of Hsp16.2 in grade 4 neoplasms indicate, that Hsp16.2 protein levels increase with the grade of the tumor. Thus, according to our findings, Hsp16.2 could be a marker whose cytoplasmic expression increases as the tumor progresses.

Current treatment modalities for malignant glioblastomas including surgery, radiotherapy and chemotherapy and their combinations are being applied with limited success [40; 41]. In order to improve the survival of brain cancer patients and to decrease the toxicity associated with systemic chemotherapy, GHRH antagonists have been developed [14; 30; 42]. Their beneficial effect in experimental cancer treatment are due to suppression of the pituitary hepatic IGF axis and the direct inhibition by the GHRH antagonists' binding to pGHRH receptors and their splice variants present on tumors [20; 24; 25; 27; 28; 43; 44; 45; 46]. Among the splice variants (SV) of pituitary GHRH receptors been detected in various human cancer cell lines, SV1 is thought to be the main functional receptor responsible for mediating the effects of GHRH and GHRH antagonists in tumors [21; 25].

The presence of both pGHRH receptors and SV1 on glioblastoma cell lines DBTRG-05 and U-87MG cell lines was demonstrated using Western blot method. Our results which showed intensive pGHRH-R expression at 47.5 kDa and less intensive SV1 expression at 39.5 in both cell lines corresponded to earlier investigations [17; 21]. In accordance with a previous study, which reported improved cell survival following treatment with GHRH [47], we also observed the enhancement of glioblastoma cell viability after exposure to GHRH(1-29)NH₂. As expected, a significant decrease in cell survival was found 48 hours after treatment with GHRH antagonists, with a slightly larger reduction with MIA-602, than with JMR-132 [47]. These findings support the view that GHRH is a growth factor in brain tumors as previously found in other tumors [27]. The diminished cell viability following GHRH treatment was caused by a rise in the number of cell deaths, which led us to investigate the apoptotic pathways. The identification of critical signaling effectors of tumor cells is of

particular importance in delineating the mechanisms of tumorigenesis that can be therapeutically targeted. Several attempts to elucidate the pathways that are triggered by GHRH and GHRH antagonists have been made. Previously, it was demonstrated that GHRH stimulates p44/42 (ERK 1/2) mitogen-activated protein kinase (MAPK) activity in somatotroph cells and in a stably transfected cell line with pGHRH receptor overexpression [48]. Furthermore, the promotion of p38 MAPK phosphorylation and the activation of the transcription factors CHOP and CREB by GHRH were reported [49; 50]. It was also found that the proliferative actions of GHRH involve ERK 1/2 and Elk-1 activation [51]. According to an earlier investigation, the modulation of p21 expression mediates the effects of GHRH analogs on cell proliferation [49]. The mechanisms of action of GHRH antagonists have likewise been investigated but the intracellular signaling mechanisms underlying their pro-apoptotic activity remain elusive. It has been demonstrated however that the GHRH antagonist-induced intracellular Ca^{2+} activation and cAMP signaling [17].

In our study using Western blot, we examined the effect of new GHRH antagonists, JMR-132 and MIA-602 on the main apoptotic pathways in DBTRG-05 and U-87MG glioblastoma cell lines. The Akt signaling pathway, which is activated by growth factors and is frequently overexpressed in cancer cells, is one of the major anti-apoptotic pathways in cells [52; 53]. We found that phosphorylation of Akt was significantly decreased in a time-dependent manner following treatment with GHRH antagonists JMR-132 and MIA-602. Akt regulates its anti-apoptotic effect by phosphorylating various effector proteins, including the glycogen synthase kinase3 β [54]. Accordingly, GSK3 β phosphorylation was decreased after 5 and 10 minutes of treatment and returned to its initial level after 30 minutes. As in previous studies, a time-dependent reduction of ERK 1/2 phosphorylation was observed after treatment with GHRH antagonists and an opposite effect was detected upon treatment with GHRH(1-29)NH₂ [51]. Although, p38 MAPK was also activated by the addition of GHRH(1-29)NH₂ to the cells, the p38 phosphorylation found after 24 hours of treatment with the GHRH antagonists was double its initial intensity.

PARP plays a central role in apoptosis as it is required for the translocation of apoptosis inducing factor from mitochondria to the nucleus [55]. The release of AIF, an inductor of chromatin condensation during apoptosis, may also be a caspase dependent process, emphasizing the relevance of caspase cleavage [56]. In accord with a previous investigation, we found that GHRH antagonists caused the cleavage of PARP and caspase-3, peaking at 24 hours in glioblastoma cells at 24 hours, whereas the addition of GHRH(1-29)NH₂ kept them in their uncleaved form [57]. The integrity of the mitochondrial membrane

system embodies a major factor against stress induced damage [58]. In order to establish whether mitochondrial mechanisms are involved in the pro-apoptotic effect of GHRH antagonists, we stained DBTRG-05 cells that were treated with GHRH(1-29)NH₂ or GHRH antagonists with the membrane potential dependent mitochondrial dye, JC-1. An intense green color and the abolition of the red fluorescence component clearly demonstrated the key role of the GHRH antagonists in the demolishing of mitochondrial membrane integrity. The exposure of glioblastoma cells to GHRH(1-29)NH₂ resulted in the retention of the red fluorescence component, indicating a preservation of the mitochondrial membrane potential. Previously, it has been shown, that the depolarization of the mitochondrial membrane results in the release of pro-apoptotic signals from the mitochondrial inter-membrane space [59]. Thus, upon exposure to GHRH antagonists we observed the release of cyt c to the cytosol and the nuclear translocation of EndoG and AIF. GHRH(1-29)NH₂ treatment did not alter the intracellular localization of these proteins. The changes in the release of pro-apoptotic proteins were reflected in the afore-mentioned caspase-3 activities. These findings provide compelling evidence, that GHRH antagonists affect cell death through the following key pro-apoptotic pathways: the reduction of phosphorylated Akt, GSK3 β and ERK 1/2, the cleavage of PARP and caspase-3 and by destabilizing the mitochondrial membrane, which in turn leads to the intracellular translocation of proteins AIF, EndoG and cyt c.

We also investigated the effect of the novel GHRH antagonist, MIA-602 on DBTRG-05 glioblastoma brain tumor *in vivo*. A considerable reduction of tumor growth by MIA-602 of 69 % was found, demonstrating a significant inhibitory effect of this potent GHRH antagonist.

As we previously noted, the treatment of glioblastoma multiforme poses a formidable challenge for current cancer therapy [60], since curative surgical resection is often not attainable due to the invasivity of the tumor [60] while the efficacy of chemotherapy is impeded by the expression of multidrug resistance genes [61] and the use of chemotherapy is limited by the systemic toxicity. Doxorubicin is a highly efficacious chemotherapeutic agent in malignant glioma *in vivo* and *in vitro* [62; 63; 64]. However, due to the toxicity of doxorubicin in the traditional systemic delivery [63; 64; 65], this substance has not been an effective agent for patients with brain cancer [66]. New therapeutic strategies involve the development of drugs that reach a higher concentration at the site of the tumor, thus minimizing the systemic side-effect of the chemotherapeutic agent [63; 64; 65; 66; 67]. Somatostatin is a hypothalamic hormonal neuropeptide that inhibits the release of a variety of hormones, including growth hormone, gastrin, glucagon, insulin and pancreatic exocrine

secretion [68; 69]. Since somatostatin has a short half-life in the circulation, more stable octapeptide analogs were synthesized, such as Sandostatin by Sandoz [70] and RC-160 (vaproetide), which was developed in our laboratory [69; 71]. Five somatostatin receptor subtypes (SSTR) have been discovered [72] and the presence of SSTR2 and/or SSTR5 on various malignancies, including brain tumors [69; 73; 74; 75; 76; 77; 78; 79; 80], suggested they play a potential role in cancer therapy [73; 74; 75; 76; 77; 78; 81; 82; 83; 84; 85]. Several targeted cytotoxic hormone analogues have been synthesized in our laboratory that are hybrids of a hormonal analogue and doxorubicin [15; 86]. These cytotoxic analogues, are less toxic and more effective than free cytotoxic compounds [87]. AN-162, which is a doxorubicin linked to a somatostatin analogue, RC-160, showed promising results in experimental breast and non-small cell lung cancers [88; 89]. There is much evidence that somatostatin octapeptide analogs including the analog RC-121 the carrier of RC-160, can penetrate the blood-brain barrier. Based on these findings we determined the effect of AN-162 on DBTRG-05 glioblastoma cell line, and tested its efficacy in experimental brain tumors. We detected the expression of mRNA for somatostatin receptor (SSTR) subtypes 2 and 3 in DBTRG-05 cells with RT-PCR. Using ligand competition assay, specific high affinity receptors for somatostatin were detected. When nude mice were xenografted with DBTRG-05 glioblastoma tumors we found that AN-162 significantly inhibited tumor growth compared with the control group and the groups treated with equimolar doses of doxorubicin, somatostatin analogue RC-160 or the unconjugated mixture of doxorubicin plus RC-160. The tumor doubling time in the group of animals treated with AN-162 was extended and was significantly different from doubling times in the control group and in the other treatment groups. Our study clearly demonstrated a potent inhibitory effect of AN-162 in experimental glioblastoma, thus suggesting the possibility of its utilization in patients suffering from malignant brain cancer.

The prognosis of cancer patients is strongly correlated with the stage of the cancer at the initial diagnosis. Patients afflicted by advanced stage ovarian or breast cancer have poor prognosis and a low survival rate, since these tumors show increased invasiveness and metastatic ability [90; 91]. Malignant glioblastomas are particularly aggressive, highly angiogenic and considered to be incurable [40; 92; 93]. We conducted a set of experiments with representative cell lines from malignant glioma, breast and ovarian cancer: DBTRG-05 glioblastoma, MDA-MB-468 estrogen-independent breast cancer and ES-2 clear cell ovarian cancer cell lines.

GHRH antagonists have been found to be effective in the treatment of a variety of experimental tumors xenografted into nude mice [13; 14; 19; 20; 25; 43; 46; 94; 95; 96]. Some studies evaluated the inhibitory effect of earlier GHRH antagonists on the development of metastases *in vivo* [23; 24; 25]. We felt that it was of interest to investigate whether a new GHRH antagonist, MIA-602 is able to inhibit the invasive and metastatic activity of DBTRG-05, MDA-MB-468 and ES-2 cancer cell lines. The presence of both pGHRH receptors and SV1 on all three cancer cell lines was demonstrated using Western blot method. Our results showed an intensive pGHRH-R expression at 60 kDa and less marked SV1 expression at 39.5 in all three cell lines. The data obtained with DBTRG-05 and MDA-MB-468 cell lines corresponded to earlier investigations [21; 30]. MDA-MB-468 expressed both receptors at the highest level compared to the other two cell lines. We also demonstrated for the first time the presence of pGHRH receptors and SV1 on ES-2 ovarian cancer cells.

The process of tumor cell metastasis is a complex cascade of events, which involves numerous steps such as proliferation, separation of cells from the primary tumor, adherence of the cells to a new location, angiogenesis, the migration of cancer cells into the stroma and the proteolysis of the matrix [31; 90; 97]. It has been reported, that the impediment of local cell proliferation is the critical step in the control of metastases [97]. Previously, improved cell survival following treatment with GHRH has been demonstrated [47]. Accordingly, we investigated the inhibitory effect of MIA-602 on cell proliferation in DBTRG-05, MDA-MB-468 and ES-2 cancer cell lines. After 48 hours of treatment, 1 μ M MIA-602 decreased cell viability significantly, with similar results in all three cancer cell lines.

Tumor invasion requires both tumor cell migration and the degradation of the extracellular matrix [33]. Cell motility is one of the pivotal points of metastasis which is necessary for the tumor cell to move through the matrix and enter the circulation so that it can travel to a distant site [90]. In our study, we demonstrated that MIA-602 significantly reduces the chemotaxis of cells across a membrane toward a chemoattractant, like matrigel. Wound-healing assays showed a slower wound-closure following MIA-602 treatment, indicating decreased cancer cell motility. Cancer cell adhesion to fibronectin and matrigel was also significantly decreased after treatment with the GHRH antagonist. We also found that ES-2 showed the greatest reduction in cell adhesion and motility after treatment with MIA-602 compared to DBTRG-05 and MDA-MB-468 cell lines.

Besides the alteration of cell adhesion, tumor cell migration involves the disruption of cell-cell connections [31]. E-cadherin, the main component of intercellular adhesion, interacts with cytoskeletal proteins through the catenin complex to preserve the normal function of

epithelia [31; 33; 98; 99]. The downregulation or loss of E-cadherin in cancer cells, contributes to increased cell adhesion, cell migration and higher tumorigenicity [100; 101]. On the other hand, β -catenin released at the disruption of adherens junctions upregulates the transactivation of β -catenin-responsive genes, which has been observed in various types of cancers [102; 103]. We showed that treatment with GHRH antagonist MIA-602 resulted in the increased expression of E-cadherin and the decreased expression of β -catenin, indicating diminished tumor cell invasion. Different tumors have been reported to express caveolin-1, a constituent of caveolar membrane coats, at a lower level than normal cells [104; 105; 106]. When we exposed cancer cells to 1 μ M MIA-602, the level of caveolin-1 rose dramatically. NF- κ B is a transcriptional factor, which translocates to the nucleus to induce the transcription of proliferation, cell survival and carcinogenesis-associated genes [107; 108]. The translocation of NF- κ B to the nucleus was successfully inhibited after treatment with the GHRH antagonist, and NF- κ B showed no activation. A downstream target of NF- κ B is MMP-2. MMPs are required for the proteolysis of the extracellular matrix, facilitating the migration of cancer cells through the basal membrane [90; 109]. They constitute a family of proteases and are able to cleave different substrates of the extracellular matrix [110]. MMPs are secreted in a latent (pro-MMP) form and must be activated to reach their full proteolytic capacity [110]. The overproduction of MMP-s has been associated with tumor growth and metastasis [111; 112]. To reveal the effect of MIA-602 on cancer cell metastasis, the activity of MMP-2 and MMP-9 proteins was investigated by gelatin zymography. Originally high MMP-2 and MMP-9 activities were visible in the untreated cancer cells' supernatants. After GHRH antagonist treatment, however, their activities diminished significantly in a time-dependent manner. The results found using gelatin zymography were supported by the findings obtained with Western blot. The expression of MMP-2 was significantly reduced after the cells were treated with MIA-602. Taken together, the findings that the GHRH antagonist, MIA-602 decreases the proliferation, migration, invasion and MMP production in three cancer cell lines representing three different cancers *in vitro*, indicates its possible role as a potent tool against cancer cell metastasis.

Conclusions

1. Hsp 16.2 was detected in different types and grades of brain tumors, however, the level of expression varied according to the type and grade

of the tumor. All ninety-one tumor samples were labeled equally intranuclearly; they varied in their cytoplasmic labeling of Hsp 16.2.

2. Hsp 16.2 could not be detected in a significant quantity in normal brain tissue, it was only present in tumor cells in significant quantity and its level increased with the increase of cell anaplasia. The cytoplasmic expression of Hsp 16.2 correlates directly with the grade of the different types of brain tumors. Based on our findings, Hsp16.2 could become a valuable marker for primary brain tumor diagnosis and the anti-apoptotic activity of sHsp16.2 could become the target of drug therapy.
3. Both the pGHRH receptor and its main splice variant, SV1, were detected on the two glioblastoma cell lines, DBTRG-05 and U-87MG, pGHRH-R at 60 kDa and SV1 at 39.5 kDa.
4. GHRH antagonists, JMR-132 and MIA-602, decreased the cell viability of both DBTRG-05 and U-87MG glioblastoma cancer cell lines.
5. GHRH antagonists affect cell death through the following key pro-apoptotic pathways: the reduction of phosphorylated Akt, GSK3 β and ERK 1/2, the cleavage of PARP and caspase-3 and through the intracellular translocation of proteins AIF, EndoG and cyt c.
6. GHRH antagonists abolish mitochondrial membrane integrity, through the depolarization of the mitochondrial potential, thus leading to the release of pro-apoptotic signals from the mitochondrial inter-membrane space.
7. The treatment of experimental glioblastoma *in vivo* with the GHRH antagonist, MIA-602, resulted in the considerable (69%) reduction of tumor growth, demonstrating a significant inhibitory effect of this GHRH antagonist.
8. The new GHRH antagonist, MIA-602 decreased the proliferation, migration, invasion and MMP production in three cancer cell lines

representing three different cancers (brain, ovarian, breast cancers) *in vitro*. Exposure to MIA-602 upregulated the expression of caveolin-1 and E-cadherin, and led to the powerful downregulation of β -catenin and NF- κ B.

9. The current investigation indicates that GHRH antagonists, such as MIA-602, might be useful for the treatment of patients suffering from malignant brain cancer by the reduction of tumor growth and through the inhibition of cancer cell metastasis.

References

- [1]B. Neyns, M. D'Haeseleer, A. Rogiers, J. Van de Cauter, C. Chaskis, A. Michotte, H. Strik, The role of cytotoxic drugs in the treatment of central nervous system gliomas. *Acta Neurol Belg* 110 (2010) 1-14.
- [2]R. Stupp, M.E. Hegi, M.R. Gilbert, A. Chakravarti, Chemoradiotherapy in malignant glioma: standard of care and future directions. *J Clin Oncol* 25 (2007) 4127-4136.
- [3]E.G. Van Meir, C.G. Hadjipanayis, A.D. Norden, H.K. Shu, P.Y. Wen, J.J. Olson, Exciting new advances in neuro-oncology: the avenue to a cure for malignant glioma. *CA Cancer J Clin* 60 (2010) 166-193.
- [4]A.D. Norden, G.S. Young, K. Setayesh, A. Muzikansky, R. Klufas, G.L. Ross, A.S. Ciampa, L.G. Ebbeling, B. Levy, J. Drappatz, S. Kesari, P.Y. Wen, Bevacizumab for recurrent malignant gliomas: efficacy, toxicity, and patterns of recurrence. *Neurology* 70 (2008) 779-787.
- [5]C. Adamson, O.O. Kanu, A.I. Mehta, C. Di, N. Lin, A.K. Mattox, D.D. Bigner, Glioblastoma multiforme: a review of where we have been and where we are going. *Expert Opin Investig Drugs* 18 (2009) 1061-1083.
- [6]E. Papp, G. Nardai, C. Soti, P. Csermely, Molecular chaperones, stress proteins and redox homeostasis. *Biofactors* 17 (2003) 249-257.
- [7]Y. Sun, T.H. MacRae, The small heat shock proteins and their role in human disease. *FEBS J* 272 (2005) 2613-2627.
- [8]J. Brognard, A.S. Clark, Y. Ni, P.A. Dennis, Akt/protein kinase B is constitutively active in non-small cell lung cancer cells and promotes cellular survival and resistance to chemotherapy and radiation. *Cancer Res* 61 (2001) 3986-3997.
- [9]M. Haslbeck, sHsps and their role in the chaperone network. *Cell Mol Life Sci* 59 (2002) 1649-1657.
- [10]M. Assimakopoulou, J. Varakis, AP-1 and heat shock protein 27 expression in human astrocytomas. *J Cancer Res Clin Oncol* 127 (2001) 727-732.
- [11]M. Haslbeck, J. Buchner, Chaperone function of sHsps. *Prog Mol Subcell Biol* 28 (2002) 37-59.
- [12]A.V. Schally, J.L. Varga, J.B. Engel, Antagonists of growth-hormone-releasing hormone: an emerging new therapy for cancer. *Nat Clin Pract Endocrinol Metab* 4 (2008) 33-43.
- [13]H. Kiaris, A.V. Schally, J.L. Varga, K. Groot, P. Armatis, Growth hormone-releasing hormone: an autocrine growth factor for small cell lung carcinoma. *Proc Natl Acad Sci U S A* 96 (1999) 14894-14898.
- [14]A.V. Schally, J.L. Varga, Antagonistic Analogs of Growth Hormone-releasing Hormone: New Potential Antitumor Agents. *Trends Endocrinol Metab* 10 (1999) 383-391.
- [15]A.V. Schally, A.M. Comaru-Schally, A. Plonowski, A. Nagy, G. Halmos, Z. Rekasi, Peptide analogs in the therapy of prostate cancer. *Prostate* 45 (2000) 158-166.
- [16]A.V. Schally, K. Szepeshazi, A. Nagy, A.M. Comaru-Schally, G. Halmos, New approaches to therapy of cancers of the stomach, colon and pancreas based on peptide analogs. *Cell Mol Life Sci* 61 (2004) 1042-1068.
- [17]Z. Rekasi, T. Czompoly, A.V. Schally, F. Boldizsar, J.L. Varga, M. Zarandi, T. Berki, R.A. Horvath, P. Nemeth, Antagonist of growth hormone-releasing hormone induces apoptosis in LNCaP human

- prostate cancer cells through a Ca²⁺-dependent pathway. *Proc Natl Acad Sci U S A* 102 (2005) 3435-3440.
- [18] A.V. Schally, A.M. Comaru-Schally, A. Nagy, M. Kovacs, K. Szepeshazi, A. Plonowski, J.L. Varga, G. Halmos, Hypothalamic hormones and cancer. *Front Neuroendocrinol* 22 (2001) 248-291.
- [19] H. Kiaris, A.V. Schally, J.L. Varga, Antagonists of growth hormone-releasing hormone inhibit the growth of U-87MG human glioblastoma in nude mice. *Neoplasia* 2 (2000) 242-250.
- [20] A.V. Schally, J.L. Varga, Antagonists of growth hormone-releasing hormone in oncology. *Comb Chem High Throughput Screen* 9 (2006) 163-170.
- [21] A. Havt, A.V. Schally, G. Halmos, J.L. Varga, G.L. Toller, J.E. Horvath, K. Szepeshazi, F. Koster, K. Kovitz, K. Groot, M. Zarandi, C.A. Kanashiro, The expression of the pituitary growth hormone-releasing hormone receptor and its splice variants in normal and neoplastic human tissues. *Proc Natl Acad Sci U S A* 102 (2005) 17424-17429.
- [22] L.B. Jaeger, W.A. Banks, J.L. Varga, A.V. Schally, Antagonists of growth hormone-releasing hormone cross the blood-brain barrier: a potential applicability to treatment of brain tumors. *Proc Natl Acad Sci U S A* 102 (2005) 12495-12500.
- [23] A. Stangelberger, A.V. Schally, J.L. Varga, M. Zarandi, K. Szepeshazi, P. Armatis, G. Halmos, Inhibitory effect of antagonists of bombesin and growth hormone-releasing hormone on orthotopic and intraosseous growth and invasiveness of PC-3 human prostate cancer in nude mice. *Clin Cancer Res* 11 (2005) 49-57.
- [24] I. Chatzistamou, A.V. Schally, J.L. Varga, K. Groot, R. Busto, P. Armatis, G. Halmos, Inhibition of growth and metastases of MDA-MB-435 human estrogen-independent breast cancers by an antagonist of growth hormone-releasing hormone. *Anticancer Drugs* 12 (2001) 761-768.
- [25] G. Halmos, A.V. Schally, J.L. Varga, A. Plonowski, Z. Rekasi, T. Czompoly, Human renal cell carcinoma expresses distinct binding sites for growth hormone-releasing hormone. *Proc Natl Acad Sci U S A* 97 (2000) 10555-10560.
- [26] S. Bellyei, A. Szigeti, A. Boronkai, E. Pozsgai, E. Gomori, B. Melegh, T. Janaky, Z. Bognar, E. Hocsak, B. Sumegi, F. Gallyas, Jr., Inhibition of cell death by a novel 16.2 kD heat shock protein predominantly via Hsp90 mediated lipid rafts stabilization and Akt activation pathway. *Apoptosis* 12 (2007) 97-112.
- [27] S. Buchholz, A.V. Schally, J.B. Engel, F. Hohla, E. Heinrich, F. Koester, J.L. Varga, G. Halmos, Potentiation of mammary cancer inhibition by combination of antagonists of growth hormone-releasing hormone with docetaxel. *Proc Natl Acad Sci U S A* 104 (2007) 1943-1946.
- [28] Z. Rekasi, T. Czompoly, A.V. Schally, G. Halmos, Isolation and sequencing of cDNAs for splice variants of growth hormone-releasing hormone receptors from human cancers. *Proc Natl Acad Sci U S A* 97 (2000) 10561-10566.
- [29] H. Kiaris, A.V. Schally, R. Busto, G. Halmos, S. Artavanis-Tsakonas, J.L. Varga, Expression of a splice variant of the receptor for GHRH in 3T3 fibroblasts activates cell proliferation responses to GHRH analogs. *Proc Natl Acad Sci U S A* 99 (2002) 196-200.
- [30] N. Barabutis, A.V. Schally, Knocking down gene expression for growth hormone-releasing hormone inhibits proliferation of human cancer cell lines. *Br J Cancer* 98 (2008) 1790-1796.
- [31] J. Yu, H. Qian, Y. Li, Y. Wang, X. Zhang, X. Liang, M. Fu, C. Lin, Arsenic trioxide (As₂O₃) reduces the invasive and metastatic properties of cervical cancer cells in vitro and in vivo. *Gynecol Oncol* 106 (2007) 400-406.
- [32] K.H. Shen, S.H. Hung, L.T. Yin, C.S. Huang, C.H. Chao, C.L. Liu, Y.W. Shih, Acacetin, a flavonoid, inhibits the invasion and migration of human prostate cancer DU145 cells via inactivation of the p38 MAPK signaling pathway. *Mol Cell Biochem* (2009).
- [33] F. Su, H. Li, C. Yan, B. Jia, Y. Zhang, X. Chen, Depleting MEKK1 expression inhibits the ability of invasion and migration of human pancreatic cancer cells. *J Cancer Res Clin Oncol* (2009).
- [34] M. Li, J. Xie, L. Cheng, B. Chang, Y. Wang, X. Lan, D. Zhang, Y. Yin, N. Cheng, Suppression of invasive properties of colorectal carcinoma SW480 cells by 15-hydroxyprostaglandin dehydrogenase gene. *Cancer Invest* 26 (2008) 905-912.
- [35] A.P. Arrigo, sHsp as novel regulators of programmed cell death and tumorigenicity. *Pathol Biol (Paris)* 48 (2000) 280-288.
- [36] M. Hermisson, H. Strik, J. Rieger, J. Dichgans, R. Meyermann, M. Weller, Expression and functional activity of heat shock proteins in human glioblastoma multiforme. *Neurology* 54 (2000) 1357-1365.
- [37] A. Aoyama, R.H. Steiger, E. Frohli, R. Schafer, A. von Deimling, O.D. Wiestler, R. Klemenz, Expression of alpha B-crystallin in human brain tumors. *Int J Cancer* 55 (1993) 760-764.
- [38] T. Hitotsumatsu, T. Iwaki, M. Fukui, J. Tateishi, Distinctive immunohistochemical profiles of small heat shock proteins (heat shock protein 27 and alpha B-crystallin) in human brain tumors. *Cancer* 77 (1996) 352-361.

- [39]P. Hauser, Z. Hanzely, Z. Jakab, L. Olah, E. Szabo, A. Jeney, D. Schuler, G. Fekete, L. Bognar, M. Garami, Expression and prognostic examination of heat shock proteins (HSP 27, HSP 70, and HSP 90) in medulloblastoma. *J Pediatr Hematol Oncol* 28 (2006) 461-466.
- [40]A. Jemal, R. Siegel, E. Ward, Y. Hao, J. Xu, T. Murray, M.J. Thun, Cancer statistics, 2008. *CA Cancer J Clin* 58 (2008) 71-96.
- [41]C.A. Kanashiro, A.V. Schally, A. Nagy, G. Halmos, Inhibition of experimental U-118MG glioblastoma by targeted cytotoxic analogs of bombesin and somatostatin is associated with a suppression of angiogenic and antiapoptotic mechanisms. *Int J Oncol* 27 (2005) 169-174.
- [42]A.V. Schally, New approaches to the therapy of various tumors based on peptide analogues. *Horm Metab Res* 40 (2008) 315-322.
- [43]K. Szepeshazi, A.V. Schally, K. Groot, P. Armatis, F. Hebert, G. Halmos, Antagonists of growth hormone-releasing hormone (GH-RH) inhibit in vivo proliferation of experimental pancreatic cancers and decrease IGF-II levels in tumours. *Eur J Cancer* 36 (2000) 128-136.
- [44]R. Busto, A.V. Schally, J.L. Varga, M.O. Garcia-Fernandez, K. Groot, P. Armatis, K. Szepeshazi, The expression of growth hormone-releasing hormone (GHRH) and splice variants of its receptor in human gastroenteropancreatic carcinomas. *Proc Natl Acad Sci U S A* 99 (2002) 11866-11871.
- [45]I. Chatzistamou, A.V. Schally, J.L. Varga, K. Groot, P. Armatis, R. Busto, G. Halmos, Antagonists of growth hormone-releasing hormone and somatostatin analog RC-160 inhibit the growth of the OV-1063 human epithelial ovarian cancer cell line xenografted into nude mice. *J Clin Endocrinol Metab* 86 (2001) 2144-2152.
- [46]A. Plonowski, J.L. Varga, A.V. Schally, M. Krupa, K. Groot, G. Halmos, Inhibition of PC-3 human prostate cancers by analogs of growth hormone-releasing hormone (GH-RH) endowed with vasoactive intestinal peptide (VIP) antagonistic activity. *Int J Cancer* 98 (2002) 624-629.
- [47]R. Granata, L. Trovato, M.P. Gallo, S. Destefanis, F. Settanni, F. Scarlatti, A. Brero, R. Ramella, M. Volante, J. Isgaard, R. Levi, M. Papotti, G. Alloatti, E. Ghigo, Growth hormone-releasing hormone promotes survival of cardiac myocytes in vitro and protects against ischaemia-reperfusion injury in rat heart. *Cardiovasc Res* 83 (2009) 303-312.
- [48]P. Zeitler, G. Siriwardana, Antagonism of endogenous growth hormone-releasing hormone (GHRH) leads to reduced proliferation and apoptosis in MDA231 breast cancer cells. *Endocrine* 18 (2002) 85-90.
- [49]A.A. Volakaki, D. Lafkas, E. Kassi, A.V. Schally, A.G. Papavassiliou, H. Kiaris, Essential role of p21/waf1 in the mediation of the anti-proliferative effects of GHRH antagonist JMR-132. *J Mol Endocrinol* 41 (2008) 389-392.
- [50]G. Siriwardana, A. Bradford, D. Coy, P. Zeitler, Autocrine/paracrine regulation of breast cancer cell proliferation by growth hormone releasing hormone via Ras, Raf, and mitogen-activated protein kinase. *Mol Endocrinol* 20 (2006) 2010-2019.
- [51]R. Steinmetz, P. Zeng, D.W. King, E. Walvoord, O.H. Pescovitz, Peptides derived from pro-growth hormone-releasing hormone activate p38 mitogen-activated protein kinase in GH3 pituitary cells. *Endocrine* 15 (2001) 119-127.
- [52]O. Mistafa, U. Stenius, Statins inhibit Akt/PKB signaling via P2X7 receptor in pancreatic cancer cells. *Biochem Pharmacol* 78 (2009) 1115-1126.
- [53]N. Bardeesy, R.A. DePinho, Pancreatic cancer biology and genetics. *Nat Rev Cancer* 2 (2002) 897-909.
- [54]H. Chung, S. Seo, M. Moon, S. Park, Phosphatidylinositol-3-kinase/Akt/glycogen synthase kinase-3 beta and ERK1/2 pathways mediate protective effects of acylated and unacylated ghrelin against oxygen-glucose deprivation-induced apoptosis in primary rat cortical neuronal cells. *J Endocrinol* 198 (2008) 511-521.
- [55]Y.J. Zhao, J.H. Wang, B. Fu, M.X. Ma, B.X. Li, Q. Huang, B.F. Yang, Effects of 3-aminobenzamide on expressions of poly (ADP ribose) polymerase and apoptosis inducing factor in cardiomyocytes of rats with acute myocardial infarction. *Chin Med J (Engl)* 122 (2009) 1322-1327.
- [56]K. Ruchalski, H. Mao, S.K. Singh, Y. Wang, D.D. Mosser, F. Li, J.H. Schwartz, S.C. Borkan, HSP72 inhibits apoptosis-inducing factor release in ATP-depleted renal epithelial cells. *Am J Physiol Cell Physiol* 285 (2003) C1483-1493.
- [57]N. Barabutis, A.V. Schally, Antioxidant activity of growth hormone-releasing hormone antagonists in LNCaP human prostate cancer line. *Proc Natl Acad Sci U S A* 105 (2008) 20470-20475.
- [58]A. Tapodi, B. Debreceni, K. Hanto, Z. Bognar, I. Wittmann, F. Gallyas, Jr., G. Varbiro, B. Sumegi, Pivotal role of Akt activation in mitochondrial protection and cell survival by poly(ADP-ribose)polymerase-1 inhibition in oxidative stress. *J Biol Chem* 280 (2005) 35767-35775.
- [59]Y. Sun, M. Mansour, J.A. Crack, G.L. Gass, T.H. MacRae, Oligomerization, chaperone activity, and nuclear localization of p26, a small heat shock protein from *Artemia franciscana*. *J Biol Chem* 279 (2004) 39999-40006.

- [60]D.S. Bidros, M.A. Vogelbaum, Novel drug delivery strategies in neuro-oncology. *Neurotherapeutics* 6 (2009) 539-546.
- [61]C. Balmaceda, Advances in brain tumor chemosensitivity. *Curr Opin Oncol* 10 (1998) 194-200.
- [62]J.E. Wolff, T. Trilling, G. Molenkamp, R.M. Egeler, H. Jurgens, Chemosensitivity of glioma cells in vitro: a meta analysis. *J Cancer Res Clin Oncol* 125 (1999) 481-486.
- [63]M.S. Lesniak, U. Upadhyay, R. Goodwin, B. Tyler, H. Brem, Local delivery of doxorubicin for the treatment of malignant brain tumors in rats. *Anticancer Res* 25 (2005) 3825-3831.
- [64]T. Hekmatara, C. Bernreuther, A.S. Khalansky, A. Theisen, J. Weissenberger, J. Matschke, S. Gelperina, J. Kreuter, M. Glatzel, Efficient systemic therapy of rat glioblastoma by nanoparticle-bound doxorubicin is due to antiangiogenic effects. *Clin Neuropathol* 28 (2009) 153-164.
- [65]T. Inoue, Y. Yamashita, M. Nishihara, S. Sugiyama, Y. Sonoda, T. Kumabe, M. Yokoyama, T. Tominaga, Therapeutic efficacy of a polymeric micellar doxorubicin infused by convection-enhanced delivery against intracranial 9L brain tumor models. *Neuro Oncol* 11 (2009) 151-157.
- [66]K. Fabel, J. Dietrich, P. Hau, C. Wismeth, B. Winner, S. Przywara, A. Steinbrecher, W. Ullrich, U. Bogdahn, Long-term stabilization in patients with malignant glioma after treatment with liposomal doxorubicin. *Cancer* 92 (2001) 1936-1942.
- [67]J. Vaage, E. Barbera-Guillem, R. Abra, A. Huang, P. Working, Tissue distribution and therapeutic effect of intravenous free or encapsulated liposomal doxorubicin on human prostate carcinoma xenografts. *Cancer* 73 (1994) 1478-1484.
- [68]P. Brazeau, W. Vale, R. Burgus, N. Ling, M. Butcher, J. Rivier, R. Guillemin, Hypothalamic polypeptide that inhibits the secretion of immunoreactive pituitary growth hormone. *Science* 179 (1973) 77-79.
- [69]M.N. Pollak, A.V. Schally, Mechanisms of antineoplastic action of somatostatin analogs. *Proc Soc Exp Biol Med* 217 (1998) 143-152.
- [70]W. Bauer, U. Briner, W. Doepfner, R. Haller, R. Huguenin, P. Marbach, T.J. Petcher, Pless, SMS 201-995: a very potent and selective octapeptide analogue of somatostatin with prolonged action. *Life Sci* 31 (1982) 1133-1140.
- [71]R.Z. Cai, B. Szoke, R. Lu, D. Fu, T.W. Redding, A.V. Schally, Synthesis and biological activity of highly potent octapeptide analogs of somatostatin. *Proc Natl Acad Sci U S A* 83 (1986) 1896-1900.
- [72]G. Weckbecker, F. Raulf, B. Stolz, C. Bruns, Somatostatin analogs for diagnosis and treatment of cancer. *Pharmacol Ther* 60 (1993) 245-264.
- [73]G. Srkalovic, R.Z. Cai, A.V. Schally, Evaluation of receptors for somatostatin in various tumors using different analogs. *J Clin Endocrinol Metab* 70 (1990) 661-669.
- [74]L. Buscail, N. Delesque, J.P. Esteve, N. Saint-Laurent, H. Prats, P. Clerc, P. Robberecht, G.I. Bell, C. Liebow, A.V. Schally, et al., Stimulation of tyrosine phosphatase and inhibition of cell proliferation by somatostatin analogues: mediation by human somatostatin receptor subtypes SSTR1 and SSTR2. *Proc Natl Acad Sci U S A* 91 (1994) 2315-2319.
- [75]J.C. Reubi, J.C. Schaer, J.A. Laissue, B. Waser, Somatostatin receptors and their subtypes in human tumors and in peritumoral vessels. *Metabolism* 45 (1996) 39-41.
- [76]L. Buscail, J.P. Esteve, N. Saint-Laurent, V. Bertrand, T. Reisine, A.M. O'Carroll, G.I. Bell, A.V. Schally, N. Vaysse, C. Susini, Inhibition of cell proliferation by the somatostatin analogue RC-160 is mediated by somatostatin receptor subtypes SSTR2 and SSTR5 through different mechanisms. *Proc Natl Acad Sci U S A* 92 (1995) 1580-1584.
- [77]Y.C. Patel, M.T. Greenwood, R. Panetta, L. Demchyshyn, H. Niznik, C.B. Srikant, The somatostatin receptor family. *Life Sci* 57 (1995) 1249-1265.
- [78]T. Reisine, G.I. Bell, Molecular biology of somatostatin receptors. *Endocr Rev* 16 (1995) 427-442.
- [79]K.M. Kalkner, E.T. Janson, S. Nilsson, S. Carlsson, K. Oberg, J.E. Westlin, Somatostatin receptor scintigraphy in patients with carcinoid tumors: comparison between radioligand uptake and tumor markers. *Cancer Res* 55 (1995) 5801s-5804s.
- [80]A. Klage, K. Krause, K. Schierle, F. Steinert, H. Dralle, D. Fuhrer, Somatostatin receptor subtype expression in human thyroid tumours. *Horm Metab Res* 42 (2010) 237-240.
- [81]P. Cordelier, J.P. Esteve, C. Bousquet, N. Delesque, A.M. O'Carroll, A.V. Schally, N. Vaysse, C. Susini, L. Buscail, Characterization of the antiproliferative signal mediated by the somatostatin receptor subtype sst5. *Proc Natl Acad Sci U S A* 94 (1997) 9343-9348.
- [82]S.W. Lamberts, A.J. van der Lely, W.W. de Herder, L.J. Hofland, Octreotide. *N Engl J Med* 334 (1996) 246-254.
- [83]J.C. Reubi, J.A. Laissue, Multiple actions of somatostatin in neoplastic disease. *Trends Pharmacol Sci* 16 (1995) 110-115.
- [84]J.C. Reubi, B. Waser, J.C. Schaer, R. Markwalder, Somatostatin receptors in human prostate and prostate cancer. *J Clin Endocrinol Metab* 80 (1995) 2806-2814.

- [85]M. Luque-Ramirez, G.R. Portoles, C. Varela, R. Albero, I. Halperin, J. Moreira, A. Soto, R. Casamitjana, The efficacy of octreotide LAR as firstline therapy for patients with newly diagnosed acromegaly is independent of tumor extension: predictive factors of tumor and biochemical response. *Horm Metab Res* 42 (2010) 38-44.
- [86]B. Sun, A.V. Schally, G. Halmos, The presence of receptors for bombesin/GRP and mRNA for three receptor subtypes in human ovarian epithelial cancers. *Regul Pept* 90 (2000) 77-84.
- [87]C.G. Ziegler, J.W. Brown, A.V. Schally, A. Erler, L. Gebauer, A. Treszl, L. Young, L.M. Fishman, J.B. Engel, H.S. Willenberg, S. Petersenn, G. Eisenhofer, M. Ehrhart-Bornstein, S.R. Bornstein, Expression of neuropeptide hormone receptors in human adrenal tumors and cell lines: antiproliferative effects of peptide analogues. *Proc Natl Acad Sci U S A* 106 (2009) 15879-15884.
- [88]S. Seitz, A.V. Schally, A. Treszl, A. Papadia, F. Rick, L. Szalontay, K. Szepeshazi, O. Ortmann, G. Halmos, F. Hohla, S. Buchholz, Preclinical evaluation of properties of a new targeted cytotoxic somatostatin analog, AN-162 (AEZS-124), and its effects on tumor growth inhibition. *Anticancer Drugs* 20 (2009) 553-558.
- [89]A. Treszl, A.V. Schally, S. Seitz, L. Szalontay, F.G. Rick, K. Szepeshazi, G. Halmos, Inhibition of human non-small cell lung cancers with a targeted cytotoxic somatostatin analog, AN-162. *Peptides* 30 (2009) 1643-1650.
- [90]T.L. Larkins, M. Nowell, S. Singh, G.L. Sanford, Inhibition of cyclooxygenase-2 decreases breast cancer cell motility, invasion and matrix metalloproteinase expression. *BMC Cancer* 6 (2006) 181.
- [91]J.M. Arencibia, A.V. Schally, G. Halmos, A. Nagy, H. Kiaris, In vitro targeting of a cytotoxic analog of luteinizing hormone-releasing hormone AN-207 to ES-2 human ovarian cancer cells as demonstrated by microsatellite analyses. *Anticancer Drugs* 12 (2001) 71-78.
- [92]Y.K. Hong, D.S. Chung, Y.A. Joe, Y.J. Yang, K.M. Kim, Y.S. Park, W.K. Yung, J.K. Kang, Efficient inhibition of in vivo human malignant glioma growth and angiogenesis by interferon-beta treatment at early stage of tumor development. *Clin Cancer Res* 6 (2000) 3354-3360.
- [93]M. Arya, S.R. Bott, I.S. Shergill, H.U. Ahmed, M. Williamson, H.R. Patel, The metastatic cascade in prostate cancer. *Surg Oncol* 15 (2006) 117-128.
- [94]J.B. Engel, G. Keller, A.V. Schally, G.L. Toller, K. Groot, A. Havt, P. Armatis, M. Zarandi, J.L. Varga, G. Halmos, Inhibition of growth of experimental human endometrial cancer by an antagonist of growth hormone-releasing hormone. *J Clin Endocrinol Metab* 90 (2005) 3614-3621.
- [95]K. Szepeshazi, A.V. Schally, K. Groot, P. Armatis, G. Halmos, F. Herbert, B. Szende, J.L. Varga, M. Zarandi, Antagonists of growth hormone-releasing hormone (GH-RH) inhibit IGF-II production and growth of HT-29 human colon cancers. *Br J Cancer* 82 (2000) 1724-1731.
- [96]Z. Kahan, J.L. Varga, A.V. Schally, Z. Rekasi, P. Armatis, L. Chatzistamou, T. Czompoly, G. Halmos, Antagonists of growth hormone-releasing hormone arrest the growth of MDA-MB-468 estrogen-independent human breast cancers in nude mice. *Breast Cancer Res Treat* 60 (2000) 71-79.
- [97]L.H. Wei, K.P. Lai, C.A. Chen, C.H. Cheng, Y.J. Huang, C.H. Chou, M.L. Kuo, C.Y. Hsieh, Arsenic trioxide prevents radiation-enhanced tumor invasiveness and inhibits matrix metalloproteinase-9 through downregulation of nuclear factor kappaB. *Oncogene* 24 (2005) 390-398.
- [98]C. Jamora, E. Fuchs, Intercellular adhesion, signalling and the cytoskeleton. *Nat Cell Biol* 4 (2002) E101-108.
- [99]D.L. Rimm, E.R. Koslov, P. Kebriaei, C.D. Cianci, J.S. Morrow, Alpha 1(E)-catenin is an actin-binding and -bundling protein mediating the attachment of F-actin to the membrane adhesion complex. *Proc Natl Acad Sci U S A* 92 (1995) 8813-8817.
- [100]D. Chin, G.M. Boyle, A.J. Kane, D.R. Theile, N.K. Hayward, P.G. Parson, W.B. Coman, Invasion and metastasis markers in cancers. *Br J Plast Surg* 58 (2005) 466-474.
- [101]K. Vleminckx, L. Vakaet, Jr., M. Mareel, W. Fiers, F. van Roy, Genetic manipulation of E-cadherin expression by epithelial tumor cells reveals an invasion suppressor role. *Cell* 66 (1991) 107-119.
- [102]P.J. Morin, beta-catenin signaling and cancer. *Bioessays* 21 (1999) 1021-1030.
- [103]S.A. Vantighem, S.M. Wilson, C.O. Postenka, W. Al-Katib, A.B. Tuck, A.F. Chambers, Dietary genistein reduces metastasis in a postsurgical orthotopic breast cancer model. *Cancer Res* 65 (2005) 3396-3403.
- [104]M. Bagnoli, A. Tomassetti, M. Figini, S. Flati, V. Dolo, S. Canevari, S. Miotti, Downmodulation of caveolin-1 expression in human ovarian carcinoma is directly related to alpha-folate receptor overexpression. *Oncogene* 19 (2000) 4754-4763.
- [105]F.C. Bender, M.A. Reymond, C. Bron, A.F. Quest, Caveolin-1 levels are down-regulated in human colon tumors, and ectopic expression of caveolin-1 in colon carcinoma cell lines reduces cell tumorigenicity. *Cancer Res* 60 (2000) 5870-5878.
- [106]K. Wiechen, C. Sers, A. Agoulnik, K. Arlt, M. Dietel, P.M. Schlag, U. Schneider, Down-regulation of caveolin-1, a candidate tumor suppressor gene, in sarcomas. *Am J Pathol* 158 (2001) 833-839.

- [107]A.S. Baldwin, Jr., The NF-kappa B and I kappa B proteins: new discoveries and insights. *Annu Rev Immunol* 14 (1996) 649-683.
- [108]A. Rossi, P. Kapahi, G. Natoli, T. Takahashi, Y. Chen, M. Karin, M.G. Santoro, Anti-inflammatory cyclopentenone prostaglandins are direct inhibitors of IkappaB kinase. *Nature* 403 (2000) 103-108.
- [109]S. Curran, G.I. Murray, Matrix metalloproteinases: molecular aspects of their roles in tumour invasion and metastasis. *Eur J Cancer* 36 (2000) 1621-1630.
- [110]P.A. Snoek-van Beurden, J.W. Von den Hoff, Zymographic techniques for the analysis of matrix metalloproteinases and their inhibitors. *Biotechniques* 38 (2005) 73-83.
- [111]L.M. Coussens, B. Fingleton, L.M. Matrisian, Matrix metalloproteinase inhibitors and cancer: trials and tribulations. *Science* 295 (2002) 2387-2392.
- [112]M.J. Duffy, T.M. Maguire, A. Hill, E. McDermott, N. O'Higgins, Metalloproteinases: role in breast carcinogenesis, invasion and metastasis. *Breast Cancer Res* 2 (2000) 252-257.

Témához tartozó publikációk:

- 1: **Pozsgai E**, Schally AV, Zarandi M, Varga JL, Vidaurre I, Bellyei S. The effect of GHRH antagonists on human glioblastomas and their mechanism of action. *Int J Cancer*. 2010 Nov 15;127(10):2313-22. PubMed PMID: 20162575.
IF: 4.734
- 2: **Pozsgai E**, Schally AV, Halmos G, Rick F, Bellyei S. The inhibitory effect of a novel cytotoxic somatostatin analogue AN-162 on experimental glioblastoma. *Horm Metab Res*. 2010 Oct;42(11):781-6. Epub 2010 Jul 27. PubMed PMID: 20665426.
IF: 2.685
- 3: Kovács M, Schally AV, Hohla F, Rick FG, **Pozsgai E**, Szalontay L, Varga JL, Zarándi M. A correlation of endocrine and anticancer effects of some antagonists of GHRH. *Peptides*. 2010 Oct;31(10):1839-46. Epub 2010 Jul 13. PubMed PMID: 20633588.
IF: 2.705
- 4: Bellyei S, Schally AV, Zarandi M, Varga JL, Vidaurre I, **Pozsgai E**. GHRH antagonists reduce the invasive and metastatic potential of human cancer cell lines in vitro. *Cancer Lett*. 2010 Jul 1;293(1):31-40. Epub 2010 Jan 12. PubMed PMID: 20064686.
IF: 3.741
- 5: **Pozsgai E**, Gomori E, Szigeti A, Boronkai A, Gallyas F Jr, Sumegi B, Bellyei S. Correlation between the progressive cytoplasmic expression of a novel small heat shock protein (Hsp16.2) and malignancy in brain tumors. *BMC Cancer*. 2007 Dec 21;7:233. PubMed PMID: 18154656; PubMed Central PMCID: PMC2234428.
IF: 2.709
- 6: Bellyei S, Szigeti A, **Pozsgai E**, Boronkai A, Gomori E, Hocsak E, Farkas R, Sumegi B, Gallyas F Jr. Preventing apoptotic cell death by a novel small heat shock protein. *Eur J Cell Biol*. 2007 Mar;86(3):161-71. Epub 2007 Feb 1. PubMed

PMID: 17275951.

IF: 3.224

7: Bellyei S, Szigeti A, Boronkai A, **Pozsgai E**, Gomori E, Meleg B, Janaky T, Bognar Z, Hocsak E, Sumegi B, Gallyas F Jr. Inhibition of cell death by a novel 16.2 kD heat shock protein predominantly via Hsp90 mediated lipid rafts stabilization and Akt activation pathway. *Apoptosis*. 2007 Jan;12(1):97-112.

PubMed PMID: 17136496.

IF: 3.043

Témában Összes IF: 22.841

Egyéb publikációk:

1: Hocsak E, Racz B, Szabo A, **Pozsgai E**, Szigeti A, Szigeti E, Gallyas F Jr, Sumegi B, Javor S, Bellyei S. TIP47 confers resistance to taxol-induced cell death by preventing the nuclear translocation of AIF and Endonuclease G. *Eur J Cell Biol*. 2010 Nov;89(11):853-61. Epub 2010 Aug 12. PubMed PMID: 20708296.

IF: 3.314

2: Hocsak E, Racz B, Szabo A, Mester L, Rapolti E, **Pozsgai E**, Javor S, Bellyei S, Gallyas F Jr, Sumegi B, Szigeti A. TIP47 protects mitochondrial membrane integrity and inhibits oxidative-stress-induced cell death. *FEBS Lett*. 2010 Jul 2;584(13):2953-60. PubMed PMID: 20556887.

IF: 3.541

3: Papp A, Cseke L, Farkas R, Pavlovics G, Horvath G, Varga G, Szigeti A, Bellyei S, Marton S, Poto L, Kalmar K, Vereczkei A, **Pozsgai E**, Horvath OP.

Chemo-radiotherapy in locally advanced squamous cell oesophageal cancer--are upper third tumours more responsive? *Pathol Oncol Res*. 2010 Jun;16(2):193-200.

Epub 2009 Sep 17. PubMed PMID: 19760123.

IF: 1.152

4: Szigeti A, Hocsak E, Rapolti E, Racz B, Boronkai A, **Pozsgai E**, Debreceni B, Bognar Z, Bellyei S, Sumegi B, Gallyas F Jr. Facilitation of mitochondrial outer and inner membrane permeabilization and cell death in oxidative stress by a novel Bcl-2 homology 3 domain protein. *J Biol Chem*. 2010 Jan 15;285(3):2140-51. Epub 2009 Nov 9. PubMed PMID: 19901022; PubMed Central PMCID: PMC2804370.

IF: 5.520

5: Boronkai A, Bellyei S, Szigeti A, **Pozsgai E**, Bognar Z, Sumegi B, Gallyas F Jr. Potentiation of paclitaxel-induced apoptosis by galectin-13 overexpression via activation of Ask-1-p38-MAP kinase and JNK/SAPK pathways and suppression of Akt and ERK1/2 activation in U-937 human macrophage cells. *Eur J Cell Biol.* 2009 Dec;88(12):753-63. Epub 2009 Aug 31. PubMed PMID: 19717209.

IF: 3.955

6: Szigeti A, Minik O, Hocsak E, **Pozsgai E**, Boronkai A, Farkas R, Balint A, Bodis J, Sumegi B, Bellyei S. Preliminary study of TIP47 as a possible new biomarker of cervical dysplasia and invasive carcinoma. *Anticancer Res.* 2009 Feb;29(2):717-24. PubMed PMID: 19331227.

IF: 1.390

7: Szapary L, Bagoly E, Kover F, Feher G, **Pozsgai E**, Koltai K, Hanto K, Komoly S, Doczi T, Toth K. The effect of carotid stenting on rheological parameters, free radical production and platelet aggregation. *Clin Hemorheol Microcirc.* 2009;43(3):209-17. PubMed PMID: 19847055.

8: Fehér G, Bagoly E, Kövér F, Koltai K, Hantó K, **Pozsgai E**, Komoly S, Dóczy T, Tóth K, Szapáry L. [The effect of carotid stenting on rheological parameters, free radical production and platelet aggregation]. *Orv Hetil.* 2007 Dec 16;148(50):2365-70. Hungarian. PubMed PMID: 18055360.

Egyéb Összes IF: 18.872

Kumulatív IF: 41.713